ИНСТИТУТ ЯДЕРНОЙ ФИЗИКИ СО АН СССР

L.M. Barkov, D.A. Melik-Pashayev
and M.S. Zolotorev

LASER SPECTROSCOPY OF ATOMIC SAMARIUM

PREPRINT 88-142

НОВОСИБИРСК

LASER SPECTROSCOPY OF ATOMIC SAMARIUM

L.M.Barkov, D.A.Melik-Pashayev and M.S.Zolotorev
Institute of Nuclear Physics, Novosibirsk 630090, USSR

Abstract

Samarium spectrum was studied with a purpose to find transitions to be used in experiments on parity nonconservation. Macaluso-Corbino effect - Faraday rotation near resonance was used for the search and study of spectral lines. We have identified previously unknown energy levels belonging to the $4f^6 6s^2\ ^5D$ term: 15914.55(3) cm^{-1} (J=1), 17864.29(3) cm^{-1} (J=2), 20195.76(3) cm^{-1} (J=3). M1-transitions to these levels from the levels of the ground $4f^6 6s^2\ ^7F$ term were observed. There are several peculiarities of these transitions which are due to the fact that they occur within an inner $4f^6$-shell, particularly, a very small pressure broadening by inert gases.

In the course of transition identification the pressure broadening, isotope shifts, ratio of the Faraday rotation and absorption, line intensity dependences on temperature, Zeeman splitting patterns and saturation spectroscopy lineshapes were studied for a number of samarium lines. Most of these lines corresponded to E1-transitions from highly excited states.

1. Introduction

During the last decade atomic spectroscrpy has sufficiently contributed to the study of fundamental interactions between elementary particles. The existence of Parity nonconservation (PNC) in atoms was unambiguously established in several experiments carried out in bismuth, thallium, lead and cesium (for reviews see e.g. [1-5]). Still, many important aspects of PNC are to be studied in detail. Among them is the nuclear spin dependence of PNC-effects, which arises due to the anapole moment of nucleus [6,7] and the coupling of the electron vector current with axial nucleon current. This dependence can be studied by comparing the PNC-effects on different hyperfine components of a transition. It would also be interesting to determine weak charges of proton and neutron separately. A possible way to do that is to measure the difference of PNC-effects for different isotopes of the same element [8]. Since the discussed effects typically constitute contributions to the overall PNC-effects at a level of several percent, in order to study them one should sufficiently increase the sensitivity of existing experimental techniques. Another trend is a search for substances where PNC-effects are significantly enhanced.

In [8] attention was drawn to the rare-earth atoms and in particular to samarium where PNC-effects can be enhanced due to the anomalous proximity of opposite parity levels.

Samarium (Z=62) has 7 stable isotopes with mass numbers 144, 147, 148, 149, 150, 152 and 154. The two odd isotopes have nuclear spin I=7/2. They can be used for nuclear spin-dependent PNC measurements. The even isotopes with large differences of neutron numbers can be used for the nucleon weak charge measurements. By such measurements one can evaluate an important parameter of the standard model of the electroweak interactions - the $\sin^2\vartheta_W$ with a high accuracy, practically independently of atomic calculation errors [8].

One of the PNC-effects is the natural optical activity of atomic vapor. This effect is most pronounced in the vicinity of magnetic dipole (M1) transitions. To have significant optical rotation angles one generally requires normal (rather than strongly suppressed) M1-transitions.

The ground $4f^6 6s^2\ ^7F$ term of samarium (figure 1) consists of closely lying levels with total angular momentum J=0,1,...,6 [9]. M1-transitions between these levels can in principle be used in the PNC-experiments, however a certain inconvenience is that they lie in a far infrared region. Besides, there are no levels of opposite parity in their vicinity.

According to calculations [10] and experimental data [11] on the spectrum of doubly ionized samarium, one could have expected that there were several terms of $4f^6 6s^2$, based on the excited $4f^6$-shell in SmI, begining from about 14000 cm^{-1}. None of these terms had been identified. The lowest excited $4f^6 6s^2$ term is ^5D. According to the selection rules, M1-transitions between the levels of the ground ^7F term and the ^5D levels should be suppressed. However, according to estimations by I.B.Khriplovich based on the eigenfunctions from [10] and the calculation [12], the term mixing lifts this suppression and for some of the transitions the reduced matrix elements are of the order of a Bohr magneton. The $^7F \to {}^5D$ transition wavelength estimates based on the ion data and calculated reduced M1-matrix elements [12] are listed in table 1. The accuracy of the wavelength estimates is believed to be of the order of a dozen nm. Note that E2-matrix elements have also been calculated in [12]. According to this calculation, the relative E2-contributions to transition probabilities are very small: they do not exceed several percent even for the diogonal in J transitions, where the M1-amplitudes are suppressed.

The aim of this work was to find and identify M1-transitions of SmI in the spectral region accessible to cw dye lasers in view of the future PNC-experiments. As a result [13-15], we have found a number of M1-transitions and identified the $4f^6 6s^2\ ^5D_{1,2,3}$ levels. In the present publication a detailed description of the search and study of M1-transitions is presented along with some subsidiary results on isotope shifts, pressure broadening and saturation spectroscopy lineshapes for a number of other SmI transitions, including E1-transtitions from highly excited states and some unidentified lines.

Table 1. Wavelength estimates and calculated reduced matrix elements for the $4f^6 6s^2\ {}^7F \to 4f^6 6s^2\ {}^5D$ M1-transitions of SmI.

λ, nm	Ji->Jf	<i‖M1‖f> Bohr magn.	λ, nm	Ji->Jf	<i‖M1‖f> Bohr magn
470	3->4	-0.046	600	2->2	-0.026
490	4->4	0.057	620	3->2	-0.485
510	5->4	-0.335	640	0->1	0.160
520	2->3	0.056	650	1->1	-0.028
550	3->3	0.024	670	2->1	-0.467
560	4->3	-0.454	710	1->0	-0.325
580	1->2	0.102			

2. Faraday rotation apparatus and procedure

The experiment consisted in searching for weak lines in the spectrum of SmI that could not be identified according to the known energy levels. For registration of spectral lines we used the Faraday rotation of the polarization plane in the vicinity of a resonance (Macaluso-Corbino effect).

A traditional optical scheme of the spectropolarimeter (see e.g. [16]) was chosen. The layout of the device is shown in figure 2. A cw single frequency tunable dye-laser (Spectra Physics model 380A) was used as a light source. Typical output power was a few milliwatts and the radiation linewidth - less than 100 MHz. With a monomode fiber /1/ the laser beam was transmitted to an optical bench where other optical elements were situated. At the exit of the fiber an objective /2/ formed a parallel beam with a diameter about 2 mm which passed through crossed calcitum prism polarizer /3/ and analyzer /4/. Two heavy flint Faraday cells /5,6/ and the samarium cell /7/ were placed between the polarizer and analyzer. Axial magnetic field up to 100 Oe was created with a coil /8/. Faraday cell /5/ produced a 1 kHz polarization plane oscillation with an amplitude $2.2 \cdot 10^{-2}$ rad. At the analyzer the light beam was devided into two components with orthogonal polarizations - the dark and the bright beam. A silicon photodiode /9/ was used to measure the intensity

of the dark beam. The first harmonic of the photodiode signal was detected by a Phase-Sensitive Detector (PSD) and fed to the Faraday cell /6/, which completed the negative feedback loop. Value of the current through the coil of the Faraday cell /6/ was proportional to the angle of the polarization plane rotation in the samarium cell and as long as the feedback coefficient was kept sufficiently high it did not depend on the laser intensity. The photodiode /10/ was used to measure the intensity of the bright beam, which was almost all the light transmitted through the samarium cell. This signal was used to measure the absorption of the vapor. The light intensity at the input of the cell was stabilized. To do that, the light reflected from one of the surfaces of the polarizer was detected with another photodiode /11/. The signal from this photodiode was fed to one of the inputs of an amplifier-comparator, a dc bias voltage was fed to its other input. The output of the amplifier-comparator was fed to a Pockels cell-modulator /12/ which kept the light intensity constant within the level of 10^{-3} in the bandwidth of 1 kHz.

The Samarium cell was designed as follows. A metal samarium sample (in the present work samarium samples of natural isotope mixture were used) was heated in a molybdenum tube up to about 1400 K. The inner diameter of the tube was 14 mm, the vapor length - $l \approx 30$ cm. At 1400 K Sm vapor pressure is a few Torr and all the states of Sm ground term are considerably populated. The use of molybdenum was dictated by its resistance to extremely chemically active samarium melt and vapor. The molybdenum tube was inserted inside a ceramic tube. An ohmic heater was wound over the ceramic tube and covered with a thermoinsulator. 30 A 50 Hz current produced about 1 kW of heat which was sufficient to maintain the required temperature inside the central part of the cell. In order to reduce the magnetic field created by the heating current, the heater was made in the form of a double helix with the two components with counter-directed currents compensating each other. A system of diaphragms and buffer gas helium (p=10-100 Torr) were used to prevent samarium from depositing on the optical windows located at the cold ends of the tube. Two grams of samarium metal was enough for about 40 hours of operation. Note that a heat-pipe type oven could hardly be used here because of a high vapor pressure over the solid samarium: about 2 Torr at the melting point 1347 K [17]. The cold ends of

the ceramic tube were sealed with thin (160 μm) glass optical windows. The windows were made thin to make the period of etalon-type interference effects, appearing during wavelength scanning, much larger than typical width of samarium lines (several GHz).

In this work we used a laser, the frequency scanning system of which had been modified (for the purpose of another experiment). When searching for spectral lines the laser frequency was electonically scanned over the FSR of an intracavity Fabry-Perot etalon (≈75 GHz) by varying voltage on its piezo-element. Hopping between longitudinal modes of the laser cavity spaced by 200 MHz occured in this case. To study the lineshapes the etalon and the cavity were tuned simultaneously (one of the cavity mirrors was adjusted to a piezo-mount), which prevented the mode-hopping. Because no servo system was used to lock etalon to the cavity mode, the range of a smooth scan was limited to ≈2 GHz and in order to cover a spectral line a series of overlapping scans was made.

The laser scanning and data acquisition was controled by an ODRETTE microcomputer [18] through a CAMAC electronic system. Typical frequency sweeping rate was 4 GHz/sec for recording of the 75-GHz samples and 100 MHz/sec for the 2-GHz samples.

Absolute wavelengths were measured with a grid spectrometer DFS-24 with an accuracy of 0.01 nm.

Figure 3 shows a recording of a 75-GHz sample of samarium spectrum with magnetic field off (A) and with H=100 Oe (B). It is seen from the figure 3B that a continuous sequence of weak lines with peak rotation of the order of 10^{-5} rad appears in the Faraday rotation spectrum when magnetic field is applied. These are apparently E1-transitions from highly excited states. Actually, a simple estimate for the Faraday rotation angle at the line center is:

$$\varphi \sim \varkappa l \cdot \mu H/\Delta\nu .$$

Here $\varkappa$ is the absorption coefficient, μ - Bohr magneton, $\Delta\nu$ - linewidth. With $\Delta\nu \approx 1$ GHz (Doppler width) and H=100 Oe, we get $\mu H/\Delta\nu \sim 0.1$. Thus, for lines with $\varphi \sim 10^{-5}$ rad, the absorption coefficient has an order of magnitude $\varkappa \sim 10^{-5}$ cm^{-1}. From an estimate

$$\varkappa \sim N_i \alpha (\nu/\Delta\nu)(d/e)^2 ,$$

where N_i is the number density of atoms in the initial state of the transition, α - the fine structure constant, ν - transition frequency, d - transition dipole moment, e - electron charge; for an allowed E1-transition ($d \sim ea$, a - Bohr radius), one gets that $\varkappa \sim 10^{-5}$ corresponds to $N_i \sim 10^7$ cm^{-3}. According to the Boltzmann law,

$$N_i = N(1/Z)(2J_i+1)\exp(-E_i/kT)$$

($N=\Sigma N_i$; $Z=\Sigma(2J_i+1)\exp(-E_i/kT)$), for a total samarium density $N \sim 10^{15}$ cm^{-3}, $N_i \sim 10^7$ cm^{-3} corresponds to the levels at about 18000 cm^{-1}, which are in abundance in SmI.

These estimates show that E1-transitions from excited states of samarium should have given rise to numerous spectral lines with different intensities, corresponding to different initial state populations and transition amplitudes. According to the predictions for the $^7F \rightarrow {}^5D$ M1-transitions (the strongest of them were supposed to have $\varphi \sim 10$ mrad at H=100 Oe), we considered only lines with a polarization plane rotation angle $\varphi > 0.1$ mrad at 100 Oe. One of such lines is seen in figure 3B.

3. Results of wavelength scanning between 599 and 669 nm

Several sections of samarium spectrum (≈50 nm total) were scanned between 599 and 669 nm. Two laser dyes - Rhodamin B and an Oxazine 17 - based active liquid AGN-650 were used at this wavelength interval. During wavelength scanning we had to ommit spectral regions (~1 nm) close to E1-transitions from the ground term besause their intensity was so big that all the laser light was absorbed in the samarium cell. About 300 weaker spectral lines were recorded. They were devided into 6 arbitrary classes according to their relative strength. On the 6-th class lines the Faraday rotation was ~ 1 mrad with H=5 Oe. On the 1-st class lines the rotation was ≈0.1 mrad with H=100 Oe.

For the majority of lines it was possible to find in tables [9] a couple of levels, the lower of them lying below 15000 cm^{-1}, for which the energy difference corresponded to the line

wavelength and E1-transition between them was not forbidden by the selection rules. Such lines were tentatively ascribed to E1-transitions between these levels. Those of the lines that were later on studied in more detail are listed in table 2. Letter D means that the line is doubled on a 75-GHz recording (figure 4). Letter I means that isotope shift was measured on this line (section 4), R - the ratio of Faraday rotation and absorption was measured (section 5), S - a saturation spectroscopy experiment was performed (section 6), P - the pressure broadening by helium buffer gas was measured (section 7). For most of these transitions the initial state configuration is $4f^5 5d6s$ and the final state configuration is either unknown (type a), or tentatively assigned in tables [9] to $4f^5 5d6p$ (type b). One of the listed lines is identified as a transition between an odd level of $4f^5 6s6p$ and an even level of $4f^5 6s7s$ (type c).

Table 2. Some of the observed lines, identified as E1-transitions between excited states of SmI.

λ,nm	Class, comment	E_i, cm^{-1}	J_i	E_f, cm^{-1}	J_f	Type
600.98	2 DI	12846.64	3	29481.25	4	a
605.39	6 I	11406.50	3	27920.10	2	a
620.11	6 DI	11044.90	2	27166.50	3	a
621.38	6 DI	12445.35	5	28534.04	5	a
		(14920.45)	(3)	(31009.20)	(4)	a
624.81	6 DI	11406.50	3	27406.90	4	a
643.53	6 DR	13050.05	2	28585.07	3	a
643.76	6DIRSP	11877.50	4	27406.90	4	a
646.82	6 I	13050.05	2	28505.72	3	a
		(14856.20)	(5)	(30312.27)	(6)	a
651.46	6 DI	11406.50	3	26752.26	4	b
661.67	6 RSP	15039.59	2	30148.40	2	c
		(14563.98)	(4)	(29673.01)	(4)	a
663.13	3 DI	13458.46	4	28534.04	5	b
666.13	6 DIR	10801.10	1	25808.90	2	a

Three lines of the 1-st class were identified as $4f^5 6s^2 \rightarrow 4f^5 5d6s$ E2-transitions: 651.4 nm (292.58 cm^{-1}, J=1->15639.80 cm^{-1}, J=1), 660.2 nm (811.92 cm^{-1}, J=2->15955.24 cm^{-1}, J=2) and 665.5 nm (811.92 cm^{-1}, J=2->15834.60 cm^{-1}, J=3). Note that a $4f^5 6s^2$ (0 cm^{-1}, J=0)->$4f^5 5d6s$ (15639.80 cm^{-1}, J=1) transition was recently discussed in a context of possibilities of PNC-experiments [19]. For this transition the E2-amplitude vanishes and the M1-amplitude arising due to configuration and term mixing was estimated in [19] to be of the order of 10^{-2} Bohr magnetons.

About 40 of the observed lines could not be identified. Some of them had been observed in the emission spectra [20,21]. The unidentified lines are listed in table 3. The Faraday lines observed in this work are superimposed in table 3 to the emission lines of samarium obtained from the arc [20] and King furnace [21] experiments. We adduce only the atomic lines that are no more than 0.02 nm apart from those measured by us. Intensity of emission lines is given in arbitrary units. King furnace intensities are for 2900 K. Temperature classification was done by A.S.King [21]. He photographed the spectra at 2300 K, 2600 K and 2900 K. Lines appearing at 2300 K were attributed to classes I and II, class I lines did not change their intensity sufficiently at higher temperatures. Class III lines appeared at 2600 K. Class IV lines were faint at 2600 K and distinct at 2900 K. The doubled arc lines are marked by letter D in table 3. Identified lines show good agreement between the present work and King's data. On the one hand King observed almost all the lines of classes from 6 to 3 and many 2-nd and 1-st class lines. On the other hand, we registered most of the atomic lines observed by King with initial levels below 15000 cm^{-1}.

Table 3. Unclassified lines.

Faraday rotation			Emission			
λ, nm	Class	Comment	λ, nm	Arc	Furnace	Class (T)
599.39	2	D				
599.87	4		599.884	3	4	III
601.03	2		601.027	5	4	III
601.38	2	D	601.387	3	2	IV
601.90	2		601.915	2	1	IV
602.41	2					
602.43	3		602.445	8 D	10	III
603.31	2	D				
603.44	3					
603.50	3					
603.84	3		603.852#	4	5	III
605.29	4	D				
620.20	3	D				
620.87	3	D				
621.47	4	D				
623.66	2					
638.36	2	DP	638.366	4 D	4	IV
643.21	3	D				
643.53#	3	D	643.534#	150	60	II
645.20#	6	IRSP	645.208	150	30	II
645.75	6	IRSP	645.755	100	20	II
645.93	6	ISP	645.936	60	30	III
652.55	4	P	652.552	6	4	IV
652.58	4	P	652.576	2	3	IV
657.06	2	P				
658.41	4	I	658.414	15	8	III
659.27	4	P				
659.30	4	P	659.303	10	6	III
659.82	3	P				
659.84	3	D				
660.04	2	D	660.039	3	4	IV
660.31	3	P				

660.58	2	P	660.57	4	2	IV
660.71	4	D	660.717	6 D	4	IV
660.80	1	D				
661.95#	5	IRSP				
662.94	2	D				
663.41	2	P				
664.03	2	P	664.049	12	10	III
664.05	2	D	664.049	12	10	III
664.14	4	P	664.157	8	10	III
666.25	2	D				
667.89	2	P	667.91	200	2	IV
668.70	1	D				
669.26	3	D	669.257	3	4	IV

Notes:

603.852 nm - a group of lines.

643.53 nm - this line is situated to the red from a 6-th class line.

643.534 nm - King points out the existence of a faint line to the red from the main one.

645.20 nm - a possible identification is the transition between opposite parity levels 14154.30 cm^{-1}, J=4 and 29648.85 cm^{-1}, J=3 (the difference of their energies corresponds to λ=645.21 nm).

661.95 nm - this line is classified in the present work as an M1-transition (see bellow).

Judging on the intensity of different lines in the emission data, one could conclude that M1-transitions could not be observed in [20,21]. Thus the occurence of some lines in emission spectra gave an evidence that they were unidentified E1-transitions. The next step towards identification of the M1-transitions was to record detailed lineshapes of the M1-candidates and to measure their isotope shifts.

4. Isotope Shifts

Isotope Shift (IS) of spectral lines depends on the electron configurations of the initial and final states. For example, for E1-transitions from the $4f^56s^2$ ground term levels to the levels of $4f^55d6s^2$ IS is positive (higher transition frequencies correspond to heavier isotopes), whereas for transitions to $4f^56s6p$ levels IS is negative (see e.g. [22]). Examples of Faraday rotation lineshapes of E1-transitions from the ground term are shown in figure 5. One can distinctly see peaks corresponding to even samarium isotopes (154,152,150,148,144) while peaks corresponding to odd isotopes (149,147) are not distinct because of the hyperfine splitting (hfs). Relative amplitudes of the even isotope peaks follow the abundances of isotopes in a natural isotope mixture.

For heavy atoms the dominant cause of IS is usually the field effect - influence of a finite nuclear volume [23]. The field shift is proportional to the electron density at the nucleus and is thus mainly determined by the s-electrons (to a lesser extent - also by p-electrons). In $4f^56s^2$->$4f^56s6p$ transitions one of the two s-electrons goes to a p-state, the effective density of s-electrons at the nucleus decreases and negative shift arises. In $4f^56s^2$->$4f^55d6s^2$ transitions the number of s-electrons is constant, but screening of s-elestrons by a 5d-electron is smaller than screening by a 4f-electron [24] and hence the effective s-electron density at the nucleus increases giving rise to a positive shift. In the $4f^56s^2$->$4f^56s^2$ M1-transitions of our interest the number of s-electrons is constant. Estimations by V.A.Dzuba, V.V.Flambaum and O.P.Sushkov showed that excitation of the $4f^5$-shell did not change the screening and the electron density at the nucleus sufficiently and the IS of these transitions was much smaller than 1 GHz - i.e. the Doppler width of a spectral line in our case. As the hyperfine splitting for the odd isotopes was determined by the $4f^5$-electrons, for which the hfs constants were usually small (hyperfine constants for the ground term levels can be found e.g. in [25]), one could have expected that the overall splitting of the M1-lines under consideration would also be smaller than the Doppler width.

Detailed Faraday rotation lineshapes were recorded for a

number of E1-transitions from the ground term (at low samarium density), E1-transitions from the excited states and the unclassified lines. In order to determine the IS values from an experimental lineshape a computer fitting to the theoretical lineshape was performed. The fitting parameters were isotope splittings, Doppler and homogenious widths and the line amplitude. For the calculations of Faraday rotation profiles we used the formulae from [1] (see Appendix).

Figure 6 shows an example of recording of a transition from an excited state. Because the hyperfine constants were unknown, the fitting curve was calculated as a sum of the Faraday rotation curves for the even isotopes only. Two peaks corresponding to the odd isotopes are seen in the difference curve.

Though samarium is a popular object for IS studies due to its interesting nuclear properties and a rich spectrum (see e.g. [22,26-30] and references therein), most of the samarium IS experiments have addressed only the transitions from the ground term levels. An exception is the work [30], where some of the transitions from highly excited states were analyzed. In this work the laser-induced fluorescence and laser-rf double-resonance techniques and a beam of atomic samarium with discharge-population of even metastable states were used.

Isotpe shifts for the even isotopes for the E1-transitions from highly excited states and the unclassified lines, measured in the present work, are given in table 4. Unclassified lines are marked with letter U. The quoted uncertainties are mainly due to the ambiguity of "sewing together" of the 2-GHz scans and the unknown hfs for odd isotopes. Dash means that IS and hfs are completely masked by the Doppler broadening.

Results of IS measurements were treated with a King plot procedure [24]. The measured shifts were plotted versus IS in a pure $4f^56s^2$->$4f^56s6p$ transition 604.50 nm where it had been measured in an atomic beam experiment [28] with an accuracy of about 1 MHz. Examples of the King plots are shown in figure 7. From the intercepts on the King plots the mass shift contributions were derived under the assumption of small specific mass shift (SMS) in the 604.50 nm transition [28]. Mass shifts for $\Delta A=2$ are given in the last column of table 4. The mass shifts for the transitions from the excited states proved to be negative and their absolute values usually exceeded those of the normal mass

shift significantly: a simple reduced mass estimate of the normal mass shift gives for two isotopes with $\Delta A=2$ about +20 MHz.

Table 4. Isotope shifts and mass shift contributions.

λ, nm	Isotope shift (MHz) 152,154	150,154	148,154	144,154	Mass shift for $\Delta A=2$
600.98	1110(60)	3610(200)	5470(300)	6900(350)	-550(250)
605.39			1710(700)		
620.11	750(40)	2440(100)	3520(200)	5140(250)	-380(200)
621.38	670(30)		3230(200)		-630(300)
624.81	920(50)		3900(200)		-290(300)
643.76	870(50)	2860(150)	4060(150)	5960(200)	-410(200)
645.20 U	-	-	-	-	-
645.75 U	-	-	-	-	-
645.93# U	413(50)	1490(200)	2150(200)	3220(300)	-50(50)
646.82	350(50)				
651.46	1290(100)	3660(200)	5470(200)	8440(300)	20(300)
661.95#	-	-	-	-	-
663.13	1140(40)	3760(100)	5450(150)	7850(200)	-670(150)
666.13	920(40)	3060(120)	4240(200)	5870(200)	-550(150)

Notes:

645.93 nm - IS derived from the saturation spectroscopy lineshape (section 6).

661.95 nm - this line is is classified in the present work as an M1-transition (see bellow).

For all the listed E1-transitions from excited states the configuration of the lower state is $4f^6 5d6s$ (see section 3, table 2). The upper levels of the 651.46 and 666.13 nm transitions are tentatively ascribed in tables [9] to the $4f^6 5d6p$ configuration. Under the assumption that in the s->p transitions IS is negative, this configuration is ruled out as being a dominant one, since the experimental shift is positive. The same is true for the other transitions with positive shifts for which the upper level configurations are unknown. A possible upper level

configuration for these lines is $4f^6 5d^2 6s$. Some of such levels are tentatively identified in [9] in the proper energy region.

Some of the unclassified lines in accordance with predictions for $4f^6 6s^2 \rightarrow 4f^6 6s^2$ M1-transitions displayed no IS or hfs splitting. Still, for unambiguous selection of M1-transitions additional information was required.

5. Ratio of Faraday rotation and absorption

Measuring the ratio of Faraday rotation and absorption one can yield information on the angular momenta and the g values of the upper and lower states of a transition.

From the formulae for the absorption coefficient and the angle of Faraday rotation (see Appendix) for even isotopes (or when hfs is unresolved), in case of negligible pressure broadening, it can be seen that the ratio of Faraday rotation and absorption depends only on the magnetic field, Doppler width and a dimensionless quantity

$$R=g_f[J_i(J_i+1)-J_f(J_f+1)-2]+ g_i[J_f(J_f+1)-J_i(J_i+1)-2] ,$$

here g_i and g_f are the g values of the initial and the final state. For the majority of samarium transitions R values lie between -16 and +2 (different signes of R correspond to different signes of Faraday rotation). According to the well-known formula

$$g=1+[J(J+1)+S(S+1)-L(L+1)]/[2J(J+1)] ,$$

g values for all the ^7F and ^5D levels (i.e. the initial and final states of the M1-transitions of our interest) are 3/2. The R value is thus predicted to be -6 for all $^7F \rightarrow {}^5D$ transitions.

The ratio of Faraday rotation and absorption was estimated for some of the strongest transitions from the excited states and unclassified lines (table 5). R values for classified lines, calculated with the g values from [9] are also given.

Table 5. Ratio of Faraday rotation and absorption.

λ, nm	R(exp.)	R(theor.)	λ, nm	R(exp.)	R(theor.)
643.53#	-7(3)	-7.4	661.67	-10(3)	-8.1
643.76	-4(1)	-4.5	661.95#	-9(3)	
645.20	-5(2)		666.13	-1(0.2)	-0.64
645.75	-6(3)				

Notes:

643.53 nm - the main line (see note after table 3).

661.95 nm - this line is classified in the present work as an M1-transition (see bellow).

6. Saturation spectroscopy

As it was discussed above, most of the unclassified lines are apparently E1-transitions from the highly excited states. Though these transitions may have normal dipole moments, the corresponding lines in the Faraday and absorption spectra are weak due to the low population of initial states. The saturation spectroscopy technique (see e.g. [31] and references therein) can be used to separate forbidden transitions from the E1-transitions. Indeed, the saturation parameters for the E1 and M1-transitions are apart from other factors proportional to d^2 and m^2, where d and m are the electric and magnetic transition dipole moments, respectively. Analysis shows, that under typical experimental conditions nonliniar signals for the M1-transitions should be much weaker than those for the E1-transitons.

Layout of the saturation spectroscopy experiment is shown in figure 8. A beam splitter /1/ divided the laser beam into a stronger saturating beam and a weaker probe beam. The beams were directed in nearly opposite directions with an angle between them of about 10^{-3} rad and intersected in the samarium vapor cell. The intensity of the pump beam was sinusoidally modulated by a Pockels cell modulator /3/ at a frequency of 1-10 kHz. The induced modulation of the probe beam absorption was detected in the signal of a photodiode /5/ by a phase-sensitive detector

with an integration time 0.5 sec. The signal of the photodiode /5/ was also used for linear absorption measurement. The intensity of the probe beam at the entrance of the cell was stabilized by a feedback loop (see section 2) including a Pockels cell modulator /6/. Typical power of the pump beam was 0.3 mW and that of the probe beam - a few times less. The diameters of both beams were about 1 mm. The line recording procedure was described in section 2. A typical frequency sweeping rate was 100 MHz/sec.

E1-transitions from the ground term were recorded first. Figure 9 shows recordings of the 656.35 nm line ($4f^6 6s^2\ ^7F_4 \rightarrow 4f^6 6s6p\ ^7G_4$) at different pressures of He buffer gas. At pressures up to several tenth of a Torr (figure 9 A) the saturation signal was essentially Doppler-free. With the He pressure increase (figure 9 B,C) the peak width gradually increased and at several Torr reached a constant level smaller than the Doppler width. This can be explained as follows. At a low pressure when the Velocity-Changing Collisions (VCC) can be neglected, the pump beam affects only a certain velocity group and produces a narrow Bennet hole in the lower state velocity distribution. Adding the buffer gas we introduce the VCC which transmit the saturation to other velocity groups. In the extreme case of $\Gamma_{vcc} \gg \Gamma_{rel}$, where Γ_{rel} is the relaxation rate of the initial level population, the pump beam saturates all the velocity classes of the Maxwellian distribution. This corresponds to the saturation signal width equel to the Doppler width/$\sqrt{2}$ (see e.g. [32]). Note that the condition fulfilled here, $\Gamma_{vcc} \gg \Gamma_{rel}$, means that the collisional damping of the ground term levels is small. This is a particular case of the low collisional perturbation of $4f^6 6s^2$ states (see section 7).

The subsequent increase of the He pressure did not change the peak width sufficiently up to ~100 Torr (figure 9 D) where the pressure broadening of the transition started to manifest itself.

The effective saturation parameter measured as the ratio of the part of the absorbed probe beam intensity, oscillating synchroniously with the pump beam modulation, and the total absorbed probe beam intensity, was about 10^{-3}-10^{-2} for the recordings shown in figure 9 A-D.

To record the E1-transitions from excited states the cell

temperature was correspondingly increased. For these transitions narrow saturation signals were obtained even at high He pressures. Figure 10 shows an example of a Doppler-free signal with the He pressure of 70 Torr. This means that the relaxation of the initial state population, most likely due to collisional damping, occurs faster than the velocity mixing i.e. $\Gamma_{rel}>\Gamma_{vcc}$.

For all recorded E1-transitions from the excited states the saturation parameter was of the order of 10^{-3}.

The saturation spectroscopy signals were then recorded for the strongest M1-candidates 645.20, 645.75, 645.93 and 661.95 nm (figure 11 A - D). A significant absorption could be produced on these transitions. All the lines except the 661.95 nm transition displayed distinct saturation signals with saturation parameters of the order of 10^{-3}. The width of saturation signals at 75 Torr of He was significantly smaller than the Doppler width. For example, the transition 645.93 nm was seen as an asymmetric unary line in the absorption spectrum, while the saturation signal revealed typical samarium isotope structure (figure 11 C).

For the 661.95 nm transition no distinct saturation signal was observed (figure 11 D). This gave another evidence for its M1-nature.

2. Pressure broadening

In [33-36] an anomalously small pressure broadening of M1-transitions within the 4f-shells of rare earth elements was discovered. In [35-36] the pressure broadening by helium of infrared transitions between the ground term levels of samarium was reported to be of the order of 0.01 MHz/Torr (at 1400 K), which is at least 2 orders of magnitude smaller than the usual values of pressure broadening of atomic transitions. This fenomenon was explained by the screening action of the 5s, 5p and 6s-electrons on the 4f-shell.

The $4f^6 6s^2\ ^7F \rightarrow 4f^6 6s^2\ ^5D$ transitions of our interest are also related to the 4f-shell excitation. Asuming that the change of the 4f-shell radius during the excitation is insignificant, one can also expect small pressure broadening of these transitions.

In order to study the pressure broadening of samarium lines we again used the Faraday rotation technique (section 2). For a calibration of frequency intervals the transmission of a 2-GHz reference cavity was recorded simultaneously with the Faraday signal. Pressure broadening was estimated from the Faraday lineshapes when helium pressure was changed in the range 100 - 760 Torr. Typical behaviour of the Faraday signal under the pressure increase is shown in figure 12. Drastic changes in the Faraday rotation lineshape and magnitude are observed when the pressure broadening γ exceeds the Doppler width Δ_D. Note that when $\gamma>>\Delta_D$, the peak Faraday rotation falls as γ^{-2} rather than γ^{-1} for the absorption signal. Pressure broadening results are collected in table 6. Letter U marks the unidentified lines (table 3). For designations of E1-transitions from the excited states see table 2. The line 656.35 nm is an E1-transition from the ground term (g.t.) $4f^6 6s^2\ ^7F_4 \rightarrow 4f^6 6s6p\ ^7G_4$.

Table 6. Pressure broadening of samarium transitions by He buffer gas. T≈1400 K, except for the 656.35 nm transition for which T≈800 K.

λ, nm	Comment	γ/p, MHz/Torr
638.36	U #	~5
643.76	E1	2.1(5)
645.20	U	5.9(9)
645.75	U	5.2(5)
645.93	U	3.9(7)
652.55	U	3.3(5)
652.58	U	2.8(9)
656.35	E1(g.t.)	7.2(10)
657.06	U	6.9(16)
659.27	U	15(6)
659.30	U	5.8(13)
659.82	U	2.6(14)
660.31	U	15.5(20)
660.58	U	4.4(10)
661.67	E1	4.6(20)

661.95		U #	< 0.2
663.41		U	4.9(16)
664.03		U	3.7(12)
664.14		U	3.7(12)
667.89		U	2.9(10)

Notes:

638.36 nm - a group of lines.

661.95 nm - classified as an M1-transition in this work (see below). A more accurate study of pressure broadening and shift of M1-transitions is described in section 11.

All the studied lines except the 661.95 nm transition displayed pressure broadening of the order of a few MHz/Torr.

For the 661.95 nm transitions in accordance with our expectations for the $4f^5 6s^2 \rightarrow 4f^5 6s^2$ M1-transitions no signs of pressure broadening were observed up to 760 Torr of He (figure 13).

8. Identification of the M1-transitions

On the basis of the experimental data reported above one could make a conclusion that the 661.95 nm line corresponded to a $4f^5 6s^2\ ^7F \rightarrow 4f^5 6s^2\ ^5D$ transition. Indeed, this line lies in the spectral region where such transitions are expected and it has an intensity corresponding to an allowed M1-transition from the ground term, it has not been observed in the emission spectra, it displays a negligible isotope and hyperfine splitting, the measured ratio of the Faraday rotation and absorption is close to the prediction for the $^7F \rightarrow ^5D$ transitions, the saturation parameter for this line is much smaller than that for E1-transitions, and finally, this line has a very small pressure broadening which has also been predicted for transitions inside the 4f-shell.

Comparing the wavelength of the 661.95 nm line with the predicted wavelengths of M1-transitions (table 1) one could see that the closest predicted M1-transition was $^7F_2 \rightarrow ^5D_4$. Under the assumption that 661.95 nm was the J=2->J=1 transition it was possible to calculate the energy of the upper level and to predict the wavelengths of the J=0->J=1 and J=1->J=1 transitions. According to the matrix element calculations (table 1) the first of these transitions should have had the peak Faraday rotation about 4 times smaller than the J=2->J=1 transition, while the second one should have been suppressed by several orders of magnitude. Corresponding wavelength samples near 628 and 640 nm were then scanned. At 628.18 nm a line similar to the 661.95 nm transition was observed. The line showed no IS or hfs splitting and no pressure broadening was observed either. The ratio of the peak Faraday rotation for the 661.95 and 628.18 nm transitions was measured to be 4.8(0.5). In the region of 640 nm no line with similar properties was observed.

We thus have found two M1-transitions from the ground term levels to the $4f^5 6s^2\ ^5D_4$ level. In order to determine its energy with an accuracy at the level of 10^{-5}, the wavelength of the M1-transitions was measured with a Michelson intereferometer-based λ-meter IDV-2 using a single frequency Lamb-dip stabilized He-Ne laser as a reference. The energy of the level proved to be 15914.55(3) cm^{-1}.

For the search of M1-transitions to higher $4f^5 6s^2$ levels the small pressure broadening of the sought-for transitions was used explicitly. Using the Faraday rotation spectroscopy it was convenient to search for the lines at the buffer gas He pressure of several atm. At such pressure the lines with typical pressure broadening of 2-10 MHz/Torr (see table 6) were significantly broader then the Doppler width and, as it was discussed in section 7, the peak Faraday rotation on them was strongly suppressed.

As the Sm cell used in previous experiments could not be used at pressures higher than 1 atm, a new high-pressure cell was designed.

9. High-pressure cell

The high-pressure cell [15] is shown in figure 14. As in the previous design, Sm sample is heated in a molybdenum tube /1/. In order to protect molybdenum which is actively oxidated when heated in the air, the tube /1/ is inserted inside a stainless steel jacket, consisting of two flanges /2/ and a tube /3/ welded to them. The flanges /2/ are brazed to the ends of the

molybdenum tube /1/. The clearance between the jacket and the molybdenum tube is filled with an inert gas. In order to avoid mechanical stress on the jacket during the heating, a slow flow of this gas through nipples /4/ is arranged. The gas frees into the atmosrhere in the form of small bubbles through a 1-cm oil lock which ensures the pressure constancy in the clearance. A bellows /5/ compensates for the difference of thermal expansion of the steel jacket and the molybdenum tube. Over the tube /3/ there is an electric-porcelain tube /6/ with a resistance heater /7/ wound on it. The heater is of a double helical form to reduce the magnetic field generated by the heating current. Over the thermoinsulation /8/ there is a water-cooled stainless-steel jacket /9/. The flanges /2/ are also water-cooled. The end-pieces /10/ are sealed to them. On the end-pieces there are 3 mm - thick quarts windows /11/ and the gas leads /12/ which are used for blowing the inner volume of the cell through and filling it with a buffer gas. The cell can be operated with a buffer gas pressure in the range 1-20 atm and the temperature of the central part (l≈30 cm) up to 1500 K. Magnetic field is produced by a coil /13/.

10. Further search and identification of M1-transitons

The search for new lines was performed in the wavelength range 550-630 nm with a magnetic field H≈100 Oe and a helium pressure 1.5-5 atm. Found were previously unreported lines with small pressure broadening 611 nm and 569 nm and also a very weak line 586 nm. For all these lines isotope and hyperfine splitting was smaller than the Doppler width. It was impossible to classify these transitions using the known Sm energy levels [9]. The differences of their wavelengths corresponded to the energy intervals between the levels $^7F_3$, $^7F_4$ and $^7F_2$ of the ground term, their positions and intensities fitted the theoretical estimates (table 1) for transitions from the ground term levels to the $4f^56s^2$ $^5D_2$ level. Thus these transitions could be identified as M1-transitions from the ground term to a common $4f^56s^2$ $^5D_2$ level. Its energy was measured to be 17864.29(3) cm^{-1}.

Also found was a transition 558 nm with a small pressure broadening, isotope and hyperfine splitting. According to the predictions (table 1) a $^7F_4 \rightarrow {}^5D_3$ transition could be anticipated in this wavelength region. Supposing that the line 558 nm corresponded to this transition and adding the measured transition energy to the energy of the initial level, one obtained that the energy of the $4f^56s^2$ $^5D_3$ level was 20195.76 cm^{-1}. However, there were several reasons, why the involved supposition was not obvious and thus needed a varification. Firstly, because the wavelengths shorter than 550 nm were not accessible to our laser, no "partner", i.e. a transition to the same upper level from another ground term level had been observed for the 558 nm line. Secondly, the transition energy coinsided within the limits of accuracy with the energy difference between two highly excited states of opposite parity: 14202.85 cm^{-1} ($4f^55d6s$ $^5D_3$) and 32125.53 cm^{-1} (J=4). Thirdly, taking into account the calculation for Sm++ ion [10], one could expect in this wavelength region not only the $^7F_4 \rightarrow {}^5D_3$ transition, but also some transitions to other $4f^56s^2$ levels belonging to the terms ^5L and ^5G. Nothing was known about the intensity of such transitions.

In order to determine, whether the observed transition originated from the ground term or from an excited state, the line intensity dependences on the cell temperature for different transitions were compared. Due to the Boltzmann factor in the initial state populations, transitions from the ground term and the excited states should have displayed considerable differences in these dependences. Also taking into account the temperature dependence of samarium vapor pressure, one could have expected that with a small temperature change, the relative intensity of transitions from the levels at about 14000 cm^{-1} should have varied twice as that of transitions from the ground term.

The temperature dependences of line intensities were compared as follows. Had the cell reached its temperature steady-state, the heater was switched off and the dependence of the Faraday rotation angle on time for a certain line was recorded. Then the cell was heated again and the procedure was repeated for another line. Measurements showed that the intensity of transitions from ≈14000 cm^{-1} dropped by a factor of two in ≈80 s, while that for the M1-transitions from the ground term - in ≈150 s. The temperature dependence for the line 558 nm corres-

ponded to the dependence for M1-transitions, thus indicating that it was a transition from the ground term.

For the upper term identification an advantage was taken of a specific Zeeman-splitting pattern characteristic of the ^7F->^5D transitions. As for all these transitions the g values of the upper and lower states are equel to 1.5, a longitudinal magnetic field H splits them into two components with energies separated by 3μH. It is easy to verify that all transitions between the ground term levels and the ^5L and ^5G levels have significantly different structure and size of the splitting.

The Zeeman splitting was observed by the Faraday rotation lineshape with H≈700 Oe (μH≈Doppler width). An additional magnetic coil was introduced to produce such a field. The observed splitting for the 558 nm transition was analogous to the splitting of the $^7F_4$->$^5D_2$ transition 569 nm (figure 15) and coinsided with the calculated one (a Faraday rotation lineshape formula for the case of an arbitrary longitudinal magnetic field is given in the Appendix). Consequently, the upper state of the 558 nm transition belongs to the ^5D term and its most probable identification is the $4f^56s^2$ $^7F_4$->$4f^56s^2$ $^5D_3$.

Thus three of five $4f^56s^2$ ^5D levels (J=1,2,3) have been identified by now. Note that to search for transitions to the levels with J=0,4 one requires light sources operating in the wavelength regions about 700 and 450-520 nm, respectively.

The wavelengths (in air) of all found M1-transitions extrapolated to the zero buffer gas pressure, angular momenta of the lower and upper states and the relative values of the Faraday rotation (F) are given in the first three columns of table 7. The convention is that for the strongest transition 662 nm, F=1000. It is necessary to note that because we had to use different laser dyes for different transitions (AGN-650 for the lines 662 and 628 nm, Rhodamin 6G for the lines 611 and 586 nm, Rhodamin 110 for the lines 569 and 558 nm), they were observed in separate experimental runs. Thus the relative Faraday rotation for them is given only roughly.

11. Pressure broadening and shift of the M1-transitions

The pressure broadening γ of the found transitions was determined from the Faraday rotation lineshapes in a low magnetic field (see Appendix), recorded at buffer gas pressures in the range 1-15 atm. Frequency markers produced by a confocal thermostabilized interferometer covered with a sealed jacket were used for the frequency scale calibration and determination of the pressure shift Δ.

In order to take into account the small unknown isotope and hyperfine structure of the found transitions, the approximating curve was calculated as a sum of rotation on two close isolated lines (effective isotopes). The spacing between them was one of the fitting parameters. Model calculations showed that the values of γ and Δ were not sensitive to the details of the line splitting. The best fitting curves (figure 16) were used to measure the linewidths and positions of line centers. Thus measured parameters γ and Δ within experimental uncertainties linearly depended on the buffer gas pressure. The values of broadening and shift by helium are given in two last columns of table 7.

Table 7. Wavelengths (in air), relative values of the Faraday rotation (F), broadening γ/p and shift Δ/p by helium of the $4f^56s^2$ ^7F->$4f^56s^2$ ^5D transitions of SmI. T=1400(100) K.

λ, nm	Ji->Jf	F, rel.u.	γ/p, MHz/Torr	Δ/p, MHz/Torr
661.954	2->1	1000	0.18(2)	-0.17(2)
628.183	0->1	200	0.17(2)	-0.16(1)
610.528	3->2	400	0.20(2)	-0.20(3)
586.267	2->2	1	<0.8	-0.22(8)
568.940	1->2	40	0.18(5)	-0.20(2)
557.799	4->3	70	0.58(6)	-0.25(3)

For the 569 nm transition the pressure broadening by xenon $\gamma/p=0.53(4)$ MHz/Torr was also measured. In this measurement the xenon pressure varied in the range 1-3.5 atm. At higher pressures a strong convection started in the cell and the laser beam could not pass through it.

A comparison of the Faraday rotation curves, recorded at a constant buffer gas pressure and at different temperatures shows that under our experimental conditions (several Torr of Sm) the self-broadening and shift are negligible ($\gamma/p(Sm)<30$ MHz/Torr, $|\Delta/p(Sm)|<50$ MHz/Torr).

The obtained pressure broadening of the M1-transitions by inert gases is at least an order of magnitude smaller than typical broadening of transitions in the outer shells of atoms, in particular of samarium [37]. On the other hand, it exceeds by an order of magnitude the broadening of infrared transitions inside the samarium ground term [35-36].

Note that the lineshape formulae used in this work (Appendix), though providing a rather fair fitting of the experimental curves, incorporate only the simplest model of the pressure broadening phenomena. In particular, it does not take into account the so-called phase memory effects. In situations when the phase of the oscillating dipole moment is not smeared, while the velocity of an active atom is changed by velocity-changing collisions, lineshape perturbations occur. The phase memory effects may even lead to narrowing rather than broadening of a line (Dicke effect [38]). Generally, M1-transitions in the screened shells of the rare earth elements with a small pressure broadening are promising objects for the search and study of such effects [38,33]. In view of that, we considered the influence of the phase-memory effects on the Faraday rotation lineshapes and tried to use the modified lineshapes for the approximation of the experimental curves. Unfortunately, the pressure broadening of the M1-transitions found in this work did not prove to be small enough for the phase-memory effects to be traced at the level of experimental uncertainties.

12. Discussion

The primary aim of this work was to find M1-transitions to be used in the PNC-experiments. Figure 17 shows the ground term levels, the found $4f^6 6s^2\ ^5D$ levels with the levels of opposite parity lying close to them and the M1-transitions observed in this work.

The nuclear spin independent weak interaction mixes atomic states of opposite parity with the same total angular momentum. For all the found levels such states lie in about 200 cm^{-1} from them. Comparing this with a typical energy gap between mixing states in the atoms where PNC-effects have already been observed (~30000 cm^{-1}), one can anticipate a significant enhancement of the PNC-effects in samarium. Note, that the found M1-transitions with large amplitudes can be used in the natural optical rotation experiments, while the weaker ones (e.g. 1->1, 2->2) - in the experiments on the optical rotation in the crossed E and B fields [19], or the PNC-Stark-induced interference experiments of the type carried out in Cs and Tl [1-5].

The nuclear spin dependent weak interaction also mixes opposite parity states with total electron angular momenta differing by unity (see e.g. [1]). This interaction can be detected by comparing PNC-effects on different hfs components of a transition. Of interest in this respect could be the transitions to the $4f^6 6s^2\ ^5D_2$ level which has an opposite parity level with J=3 in 33 cm^{-1} from it. However, as it was pointed out in [8], a serious shortcoming here is the small hyperfine splitting of the $4f^6 6s^2$ levels [25]. This drawback could be on principle overcome by utilizing Doppler-free techniques, e.g. an atomic beam.

It is necessary to note that a small energy gap between the opposite parity levels does not by itself guarantee a large PNC-mixing, since the mixing coefficient also incorporates the actual PNC matrix elements which are difficult to calculate here due to a complex structure of the levels involved. Therefore, the feasibility of precision PNC-experiments with the found samarium transition should be tested by some auxiliary measurements (e.g. measurements of Stark polarizabilities) that will help to evaluate the mixing coefficients, and/or by the PNC-measurements themselves.

It is possible to suggest that apart from the vicinity of

opposite parity levels, other properties of the new levels and transitions will also prove to be useful. Firstly, the small pressure broadening of transitions inside the $4f^6 6s^2$ provides a simple method of selecting them from other spectral lines. With the tunable lasers existing today it will be possible to access M1-transitions coupling the ground term with the $^5D_{0,4}$ levels (see table 1). Transitions to some of the other terms of $4f^6 6s^2$ (^5L, ^5G, ^5H, ^5I, ^5F, ^3P, ^5K) can probably be found in the same fashion. Note that in the tables [9] there are three levels at about 30000 cm^{-1} tentatively identified as belonging to the $4f^6 6s^2$ configuration. M1-transitions from the ground term to these levels lye within the spectral range accessible to the second harmonic of dye lasers.

According to [39], only about one third of the 3500 SmI lines observed in the spectral range 260-4100 nm have been classified. Hopefully, the identification of new levels will lead to a more complete classification of samarium spectra.

The $4f^6 6s^2 \rightarrow 4f^6 6s^2$ transitons with relatively low collisional perturbation and isotope and hyperfine splitting can probably be also used as the secondary frequency standards over a wide spectral range, e.g. the $^7F \rightarrow ^5D$ transitions embrace the whole visible spectrum.

13. Summary and outlook

Samarium spectrum was studied with a purpose to find new M1-transitions to be used in the PNC-experiments. Faraday rotation technique was chosen for the search and study of spectral lines. Due to its high sensitivity this technique allowed to observe weak lines with $\varkappa L \sim 10^{-4}$. Initially the spectrum scanning was made with a helium buffer gas pressure in the vapor cell of the order of 10-100 Torr. In this case a large number of spectral lines of different intensities was observed (~10 lines per nm). Most of the observed lines were identified as E1-transitions from the ground term or from the highly excited states (intensity of these two types of transitions differed by many orders of magnitude). Some of the weak lines could not be classified. For the purpose of classification, the isotope shifts, ratio of the Faraday rotation and absorption, saturation spectroscopy lineshapes and the pressure broadenings were studied on

different samarium transitions. As a result, transitions to the $4f^6 6s^2$ $^5D_4$ level were revealed. One of the most striking features of these transitions was a very small pressure broadening. In the search for transitions to other $4f^6 6s^2$ levels an advantage of this was taken. A special samarium vapor cell was designed which allowed operation with buffer gas pressures of several atm. At such pressures most of the Faraday rotation lines were significantly broadened and suppressed in amplitude, which made it very easy to select the sought-for M1-transitions. Tests of the correctness of transition identification were provided by studying the dependences of line intensities on the cell temperature and the Zeeman splittings at high magnetic fields. This proved to be especially useful in the case of the $^7F_4 \rightarrow ^5D_3$ transition, for which no "partner" transition from another ground term level was observed. The small pressure broadenings and shifts of the found M1-transitions were then studied.

In conclusion, the new $4f^6 6s^2$ $^7F \rightarrow 4f^6 6s^2$ ^5D M1-transitions of SmI (as well as other transitions inside the 4f-shell) have many specific spectroscopic properties and will probably be used in a number of applications.

Acknowledgements

We are grateful to I.B.Khriplovich for the suggestion to start this work and for numerous helpful discussions. We are indebted to V.A.Dzuba, V.V.Flambaum, A.Ya.Kraftmakher and O.P.Sushkov for their calculations and many interesting discussions, P.L.Chapovsky for his stimulating interest in this work and a suggestion to use the saturation spectroscopy technique to separate the M1 and E1-transitions, B.A.Knyazev, V.N.Kulyasov, L.Young and A.M.Shalagin for helpful discussions, V.P.Cherepanov, A.V.Ledenev, G.S.Piskunov and S.V.Tararyshkin for their help in arranging electronics, S.D.Belov, V.R.Kozak and E.A.Simonov who contributed to the software, V.P.Smakhtin for his help in the oven design, B.V.Bondarev for providing optics for the laser, and finally, to S.A.Abramov, M.V.Remnyov and M.B.Sultanov for providing the λ-meter. The technical assistance of V.I.Sverdlov, V.M.Boreiko and V.S.Mel'nikov is acknowledged.

Appendix. Faraday rotation and absorption lineshapes

For a single line in the absence of magnetic field, in the impact approximation, one can write for the complex refractive index:

$$n-1 \propto \langle(\nu-\nu_0-\nu\beta+i\gamma/2)^{-1}\rangle=[g(u,v)-if(u,v)]/\Delta_D \ .$$

Here ν is the light frequency; ν_0 - the central frequency of the transition; β - longitudinal velocity projection, normalized by the speed of light; γ - the homogenious width (throughout this work γ is determined by collisional width); the angular brackets denote an averaging over the atomic thermal velocities; $\Delta_D=\nu_0\beta_0$ - the Doppler width ($\beta_0=(2kT/Mc^2)^{1/2}$); $u=(\nu-\nu_0)/\Delta_D$, $v=\gamma/2\Delta_D$; $g(u,v)$ and $f(u,v)$ - dimensionless functions introduced e.g. in [1]. Using this representation one gets for the absorption coefficient and the Faraday rotation angle:

$$\varkappa=4\pi N_i(2J_i+1)^{-1}\cdot(\nu/\Delta_D)\cdot|\langle f\|M\|i\rangle|^2\cdot f(u,v)/3 \ ,$$

$$\varphi/l=2\pi N_i(2J_i+1)^{-1}(\nu/\Delta_D)\ (|\mu H|/\Delta_D)(\partial g(u,v)/\partial u)\cdot|\langle f\|M\|i\rangle|^2 R/12.$$

Here N_i is the initial state population, $\langle f\|M\|i\rangle$ - the reduced matrix element of the transition (M1 or E1),

$$R=g_f[J_i(J_i+1)-J_f(J_f+1)-2] + g_i[J_f(J_f+1)-J_i(J_i+1)-2] \ .$$

These formulae are valid for small magnetic fields ($|\mu H|\ll\Delta_D$). For arbitrary fields they have to be modified as follows (O.P.Sushkov):

$$\varkappa=4\pi N_i(2J_i+1)^{-1}\cdot(\nu/\Delta_D)\cdot|\langle f\|M\|i\rangle|^2\cdot\sum_{m=-J_i}^{J_i}\begin{pmatrix}J_f & 1 & J_i\\ -m-1 & 1 & m\end{pmatrix}\cdot\frac{1}{2}[f(u-x_m)+f(u+x_m)]$$

$$\varphi/l=2\pi N_i(2J_i+1)^{-1}(\nu/\Delta_D)\cdot|\langle f\|M\|i\rangle|^2\cdot\sum_{m}\begin{pmatrix}J_f & 1 & J_i\\ -m-1 & 1 & m\end{pmatrix}\cdot\frac{1}{2}[g(u-x_m)-g(u-x_m)]$$

Here $x_m=\frac{\mu H}{\Delta_D}(g_f\cdot(m+1)-g_i\cdot m)$, $\begin{pmatrix}J_f & 1 & J_i\\ -m-1 & 1 & m\end{pmatrix}$ - a 3J-symbol [40]. Isotpe shift can be taken into account by summation over different isotopes with the relevant values of N_i and ν_0. Hyperfine splitting leads to a more complicated structure of the Faraday rotation. A corresponding discussion and formulae can be found e.g. in [1,41-43].

Note that all the Faraday rotation measurements reported in this work were made in conditions when effects nonlinear in laser power could be neglected. A special study of nonlinear Faraday rotation on samarium transitions is reported elsewhere [44].

References

[1] Khriplovich I.B. Parity Non-Conservation in Atomic Phenomena. Moscow, Nauka, 1988 (in Russian).

[2] Bouchiat M.-A. and Pottier L., in Atomic Physics 9, eds. R.S. van Dyck Jr. and E.N. Fortson, World Scientific (Singapore) 1984.

[3] Fortson E.N. and Lewis L.L.: Phys. Reports v.113, n.5 (1984), p.289.

[4] Commins E.D.: Physica Scripta v.32, (1987), p.468.

[5] Bouchiat M.-A. and Pottier L.: Science v.234 (1986), p.1203.

[6] Flambaum V.V. and Khriplovich I.B.: Zh.Eksp.Teor.Fiz. v.79 (1980), p.1656 (JETP v.52 (1980), p.835.).

[7] Flambaum V.V., Khriplovich I.B. and Sushkov O.P.: Phys. Lett. B v.146 (1984), p.367.

[8] Dzuba V.A., Flambaum V.V. and Khriplovich I.B.: Z. Phys. D v.1 (1986), p.243.

[9] Martin W.C., Zalubas R. and Hagan L. Atomic Energy Levels - The Rare-Earth Elements. Washington, NBS, 1978.

[10] Ofelt G.S.: J. Chem. Phys. v.38, n.9 (1963), p.2171.

[11] Dieke G.H. and Sarup R.: J.Chem. Phys. v.36, n.2 (1962), p.371.

[12] Kraftmakher A.Ya.: Opt. Spektrosk. (Opt.Spectrosc.USSR), in press.

[13] Barkov L.M., Zolotorev M.S. and Melik-Pashayev D.A.: Opt. Spektrosk. v.62 (1987), n.2, p.243 (Opt.Spectrosc.(USSR), v.62(2) (1987), p.144).

[14] Barkov L.M., Zolotorev M.S. and Melik-Pashayev D.A.: Kvantovaya Elektronica (Sov.J.Quant.Electron.) v.15, n.6 (1988), p.1116.

[15] Barkov L.M., Zolotorev M.S. and Melik-Pashayev D.A.: Opt. Spektrosk. (Opt.Spectrosc.USSR), in press.

[16] Birich G.N., Bogdanov Yu.V., Kanorskii S.I., Sobel'man I.I., Sorokin V.N., Struk I.I. and Yukov E.A. Precision laser spectropolarimetry. FIAN, Preprint 317, Moscow, 1986 (in Russian).

[17] Handbook on physics and chemistry of Rare Earths, v.1, eds. Karl A. Gshneider and Le Roy Eyring, North-Holland, 1978.

[18] Piskunov G.S. and Tararyshkin S.V.: Avtometriya, n.4 (1986), p.32.

[19] A Gongora T. and Sandars P.G.H.: J.Phys. B v.19 (1986), p.L291.

[20] Albertson W.: Phys. Rev. v.47 (1935), p.370.

[21] King A.S.: Astrophys. J. v.82 (1935), p.140.

[22] Striganov A.R., Katulin V.A. and Eliseyev V.V.: Opt. Spektrosk. v.12 (1962), n.2, p.171 (Opt.Spectrosc.(USSR), v.12 (1962), p.91).

[23] Heilig K. and Steudel A.: Atom. Data Nucl. Data Tables, v.14 (1974), p.613.

[24] King W.H.: J. Opt. Soc. Am., v.53 (1963), n.5, p.638.

[25] Childs W.J. and Goodman L.S.: Phys. Rev. A, v.6 (1972), n.6, p.2011.

[26] Brand H., Nottbeck B., Schulz H.H. and Steudel A.: J. Phys. B, v.11 (1978), n.4, p.L99.

[27] Griffith J.A.R., Isaak G.R., New R., Ralls M.P. and van Zyl C.P.: J. Phys. B, v.12 (1979), n.1, p.L1.

[28] Brand H., Seibert B. and Steudel A.: Z. Phys. A, v.296 (1980), p.281.

[29] Griffith J.A.R., Isaak G.R., New R. and Ralls M.P.: J. Phys. B, v.14 (1981), p.2769.

[30] Childs W.J., Poulsen O. and Goodman L.S.: Phys. Rev. A, v.19 (1979), n.1, p.160.

[31] Hansch T.W., in Atomic Physics 8, eds. Ingvar Lingren, Arne Rosen and Sune Svanberg, Plenum Press, 1983.

[32] Brechignac C., Vetter R. and Berman P.R.: Phys. Rev. A, v.17 (1978), n.5, p.1609.

[33] Aleksandrov E.B., Kotylev V.N., Vasilevskii K.P. and Kulyasov V.N.: Opt. Spektrosk. v.54 (1983), n.1, p.3.

[34] Aleksandrov E.B., Vedenin V.D. and Kulyasov V.N.: Opt. Spektrosk. v.56 (1984), n.4, p.596 (Opt.Spectrosc.(USSR), v.56 (1984), p.365).

[35] Vedenin V.D., Kulyasov V.N., Kurbatov A.L., Rodin N.V. and Shubin M.V.: Opt. Spektrosk. v.60 (1986), n.2, p.239 (Opt.Spectrosc.(USSR), v.60 (1986), p.146).

[36] Vedenin V.D., Kulyasov V.N., Kurbatov A.L., Rodin N.V. and Shubin M.V.: Opt. Spektrosk. v.62 (1987), n.4, p.737.

[37] Vedenin V.D. and Kulyasov V.N.: Opt. Spektrosk. v.59

(1985), n.5, p.1004.

[38] Dicke R.H.: Phys. Rev. v.89 (1953), n.2, p.472.

[39] Penkin N.P. and Komarovskii V.A.: J. Quant. Spectrosc. Radiat. Transfer. v.16 (1976), p.217.

[40] Sobel'man I.I. Introduction into the theory of atomic spectra. Moscow, Nauka, 1977 (in Russian).

[41] Novikov V.N., Sushkov O.P. and Khriplovich I.B.: Opt. Spektrosk. v.43 (1977), p.621; V.45 (1978), p.413.

[42] Roberts G.J., Baird P.E.G., Brimicombe M.W.S.M., Sandars P.G.H., Selby D.R. and Stacey D.N.: J. Phys. B, v.13 (1980), p.1389.

[43] Davies I.O.J., Baird P.E.G. and Nicol J.L.: J. Phys. B, v.20 (1987), p.5371.

[44] Barkov L.M., Zolotorev M.S. and Melik-Pashayev D.A. Nonlinear Faraday rotation in samarium vapor. Inst. Nucl. Phys. Preprint 88-90, Novosibirsk, 1988; Submitted to Opt. Commun.

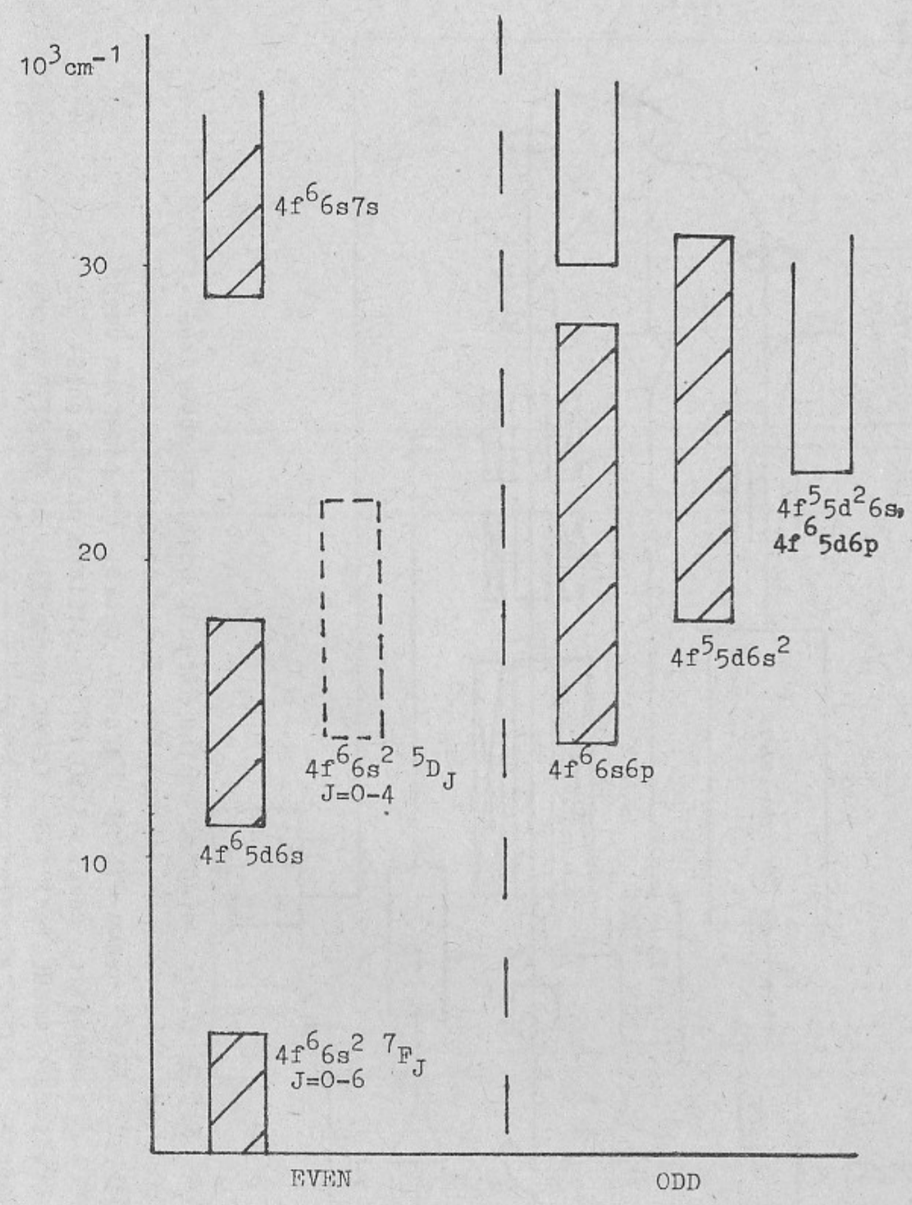

Fig.1. Samarium configurations [9].

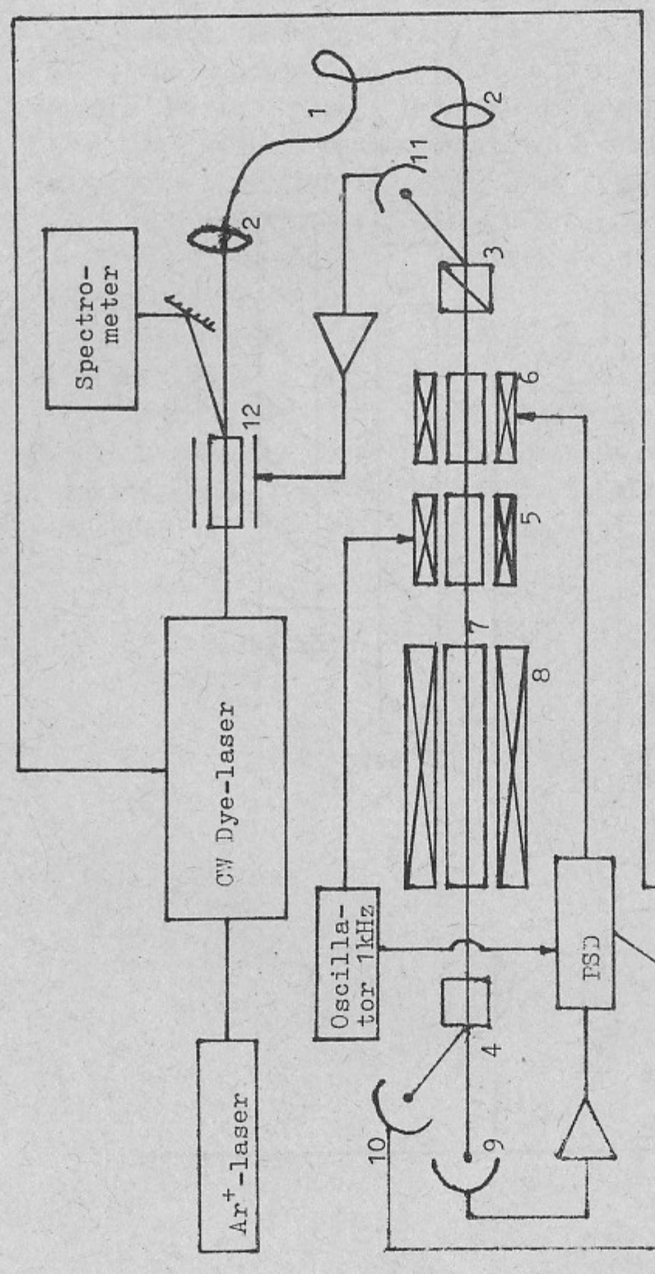

Fig.2. Block diagram of the Faraday rotation apparatus. 1 - monomode fiber; 2 - objectives; 3,4 - crossed polarizer and analyzer; 5,6 - heavy flint Faraday cells; 7 - samarium vapor cell; 8 - magnetic coil; 9,10,11 - silicon photodiodes; 12 - Pockels cell modulator; 13 - CAMAC crate with an ODRETTE micro-computer [18] as a crate-controller.

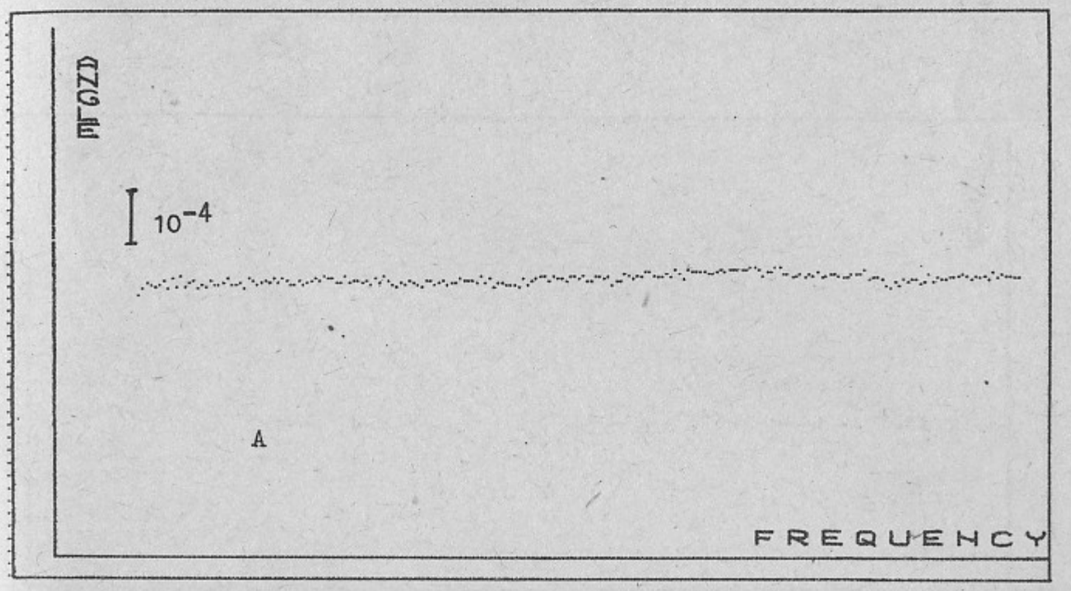

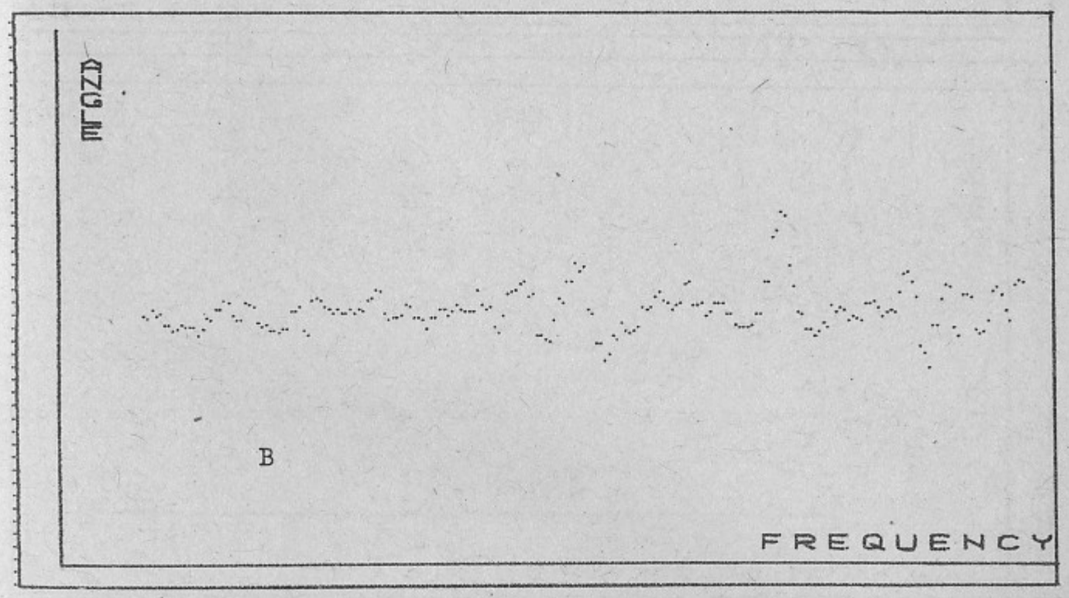

Fig.3. A - a 75-GHz sample of samarium spectrum at λ≈639.2 nm recorded with magnetic field off. B - the same sample with H=100 Oe. A continuous sequence of weak lines is seen.

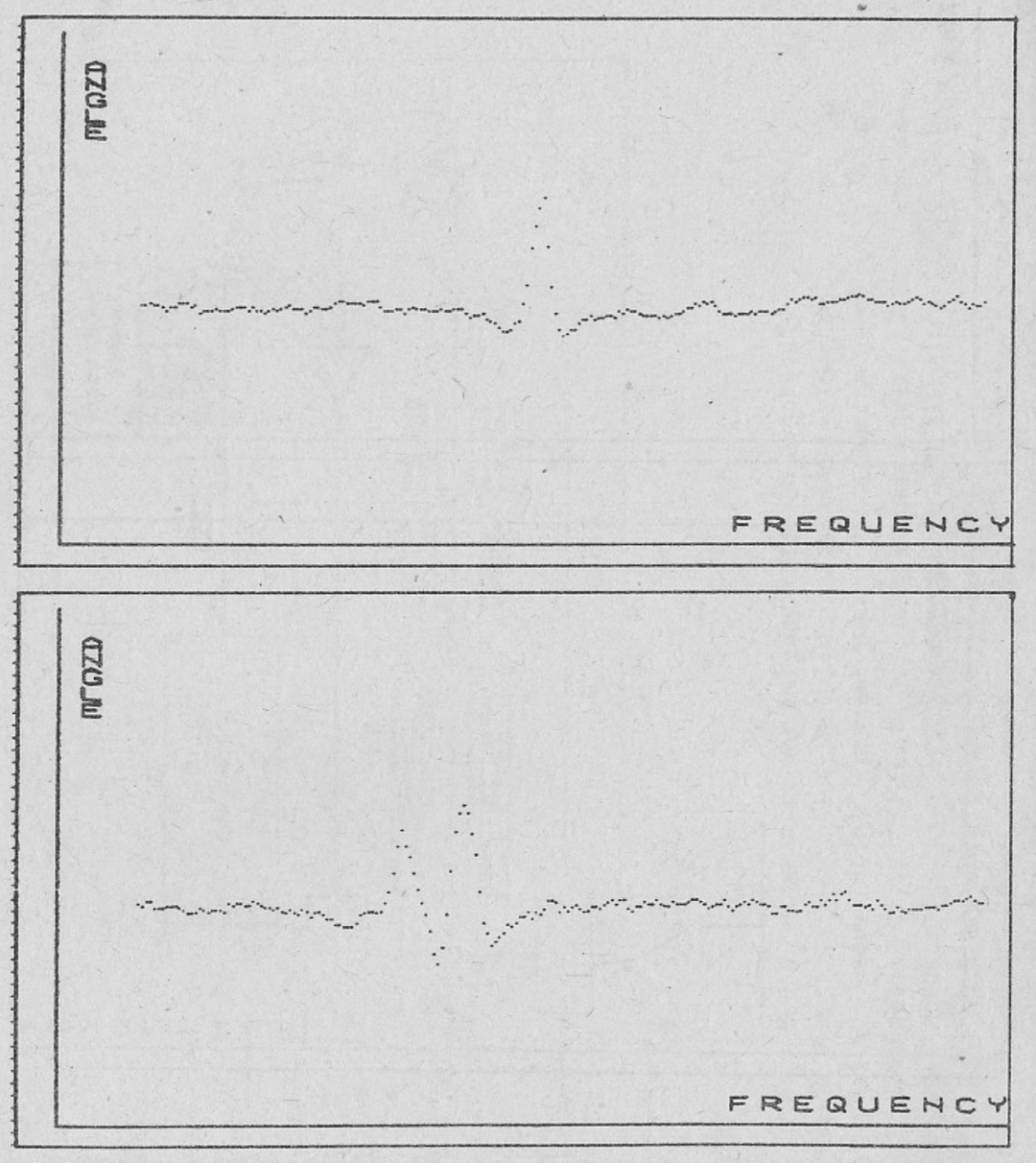

Fig.4. Examples of a unary and a doubled line on a 75-GHz recording.

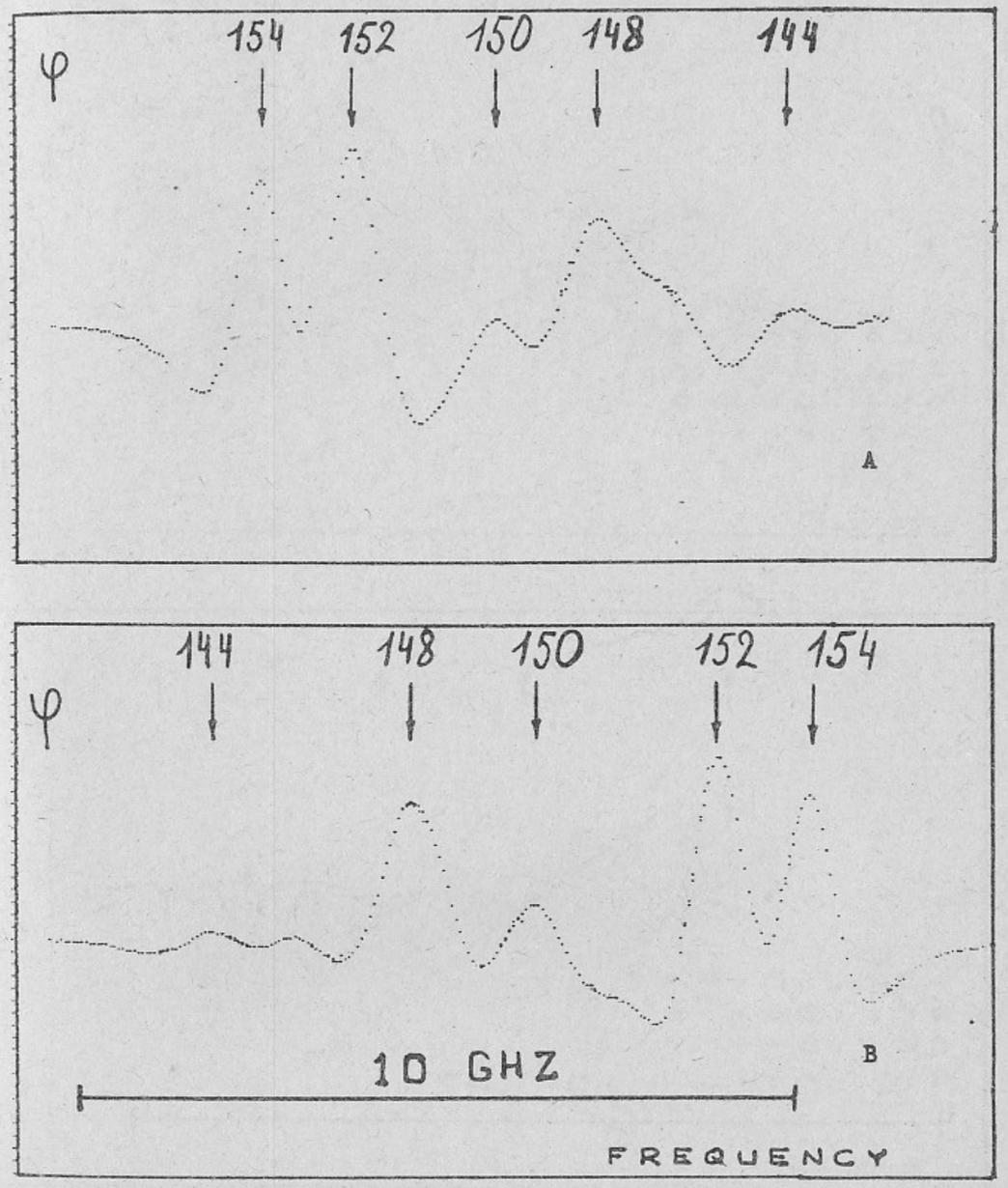

Fig.5. Detailed Faraday rotation lineshapes of E1-transitions from the ground term. Recordings were made at a low samarium pressure. A - $4f^6 6s^2 \rightarrow 4f^6 6s6p$ transtion 602.72 nm. B - a $4f^6 6s^2 \rightarrow 4f^5 5d6s^2$ transition 602.75 nm. Positions of even isotopes are marked with arrows. The two transitions have opposite IS signs.

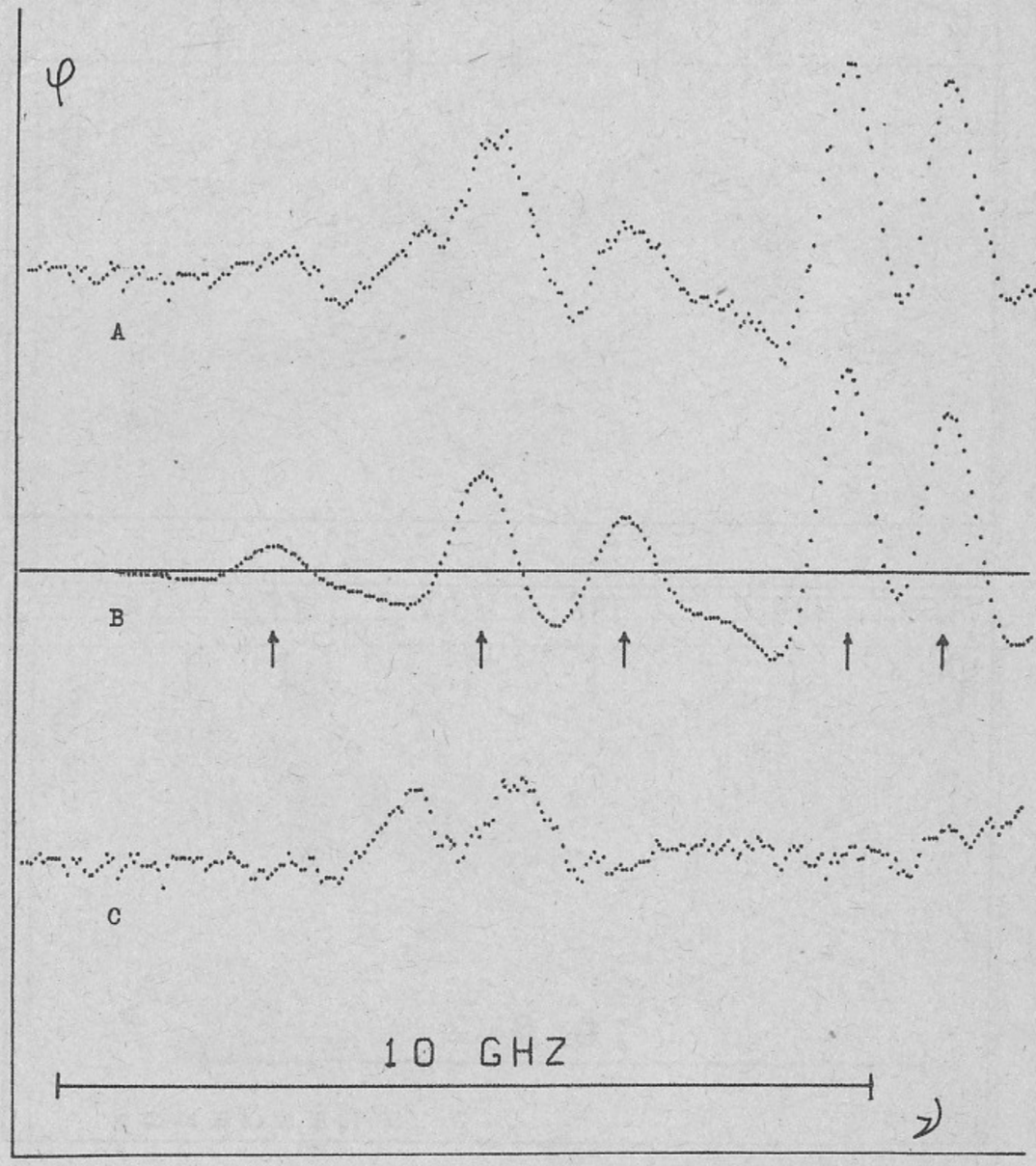

Fig.6. Faraday rotation lineshape of an E1-transition from a highly excited state 663.13 nm. A - experimental curve; B - a fitting curve. Positions of even isotopes are marked with arrows. C - difference between A and B. Two peaks on curve C correspond to odd isotopes.

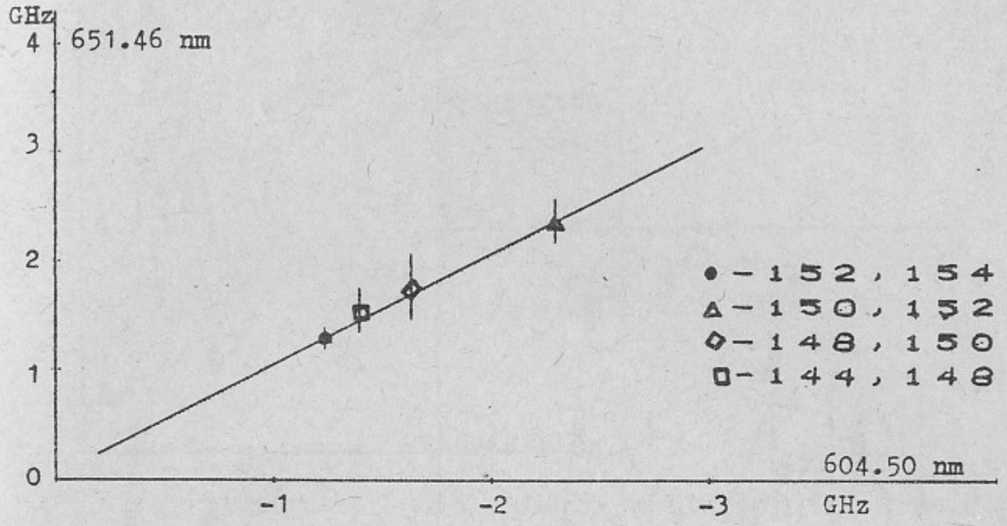

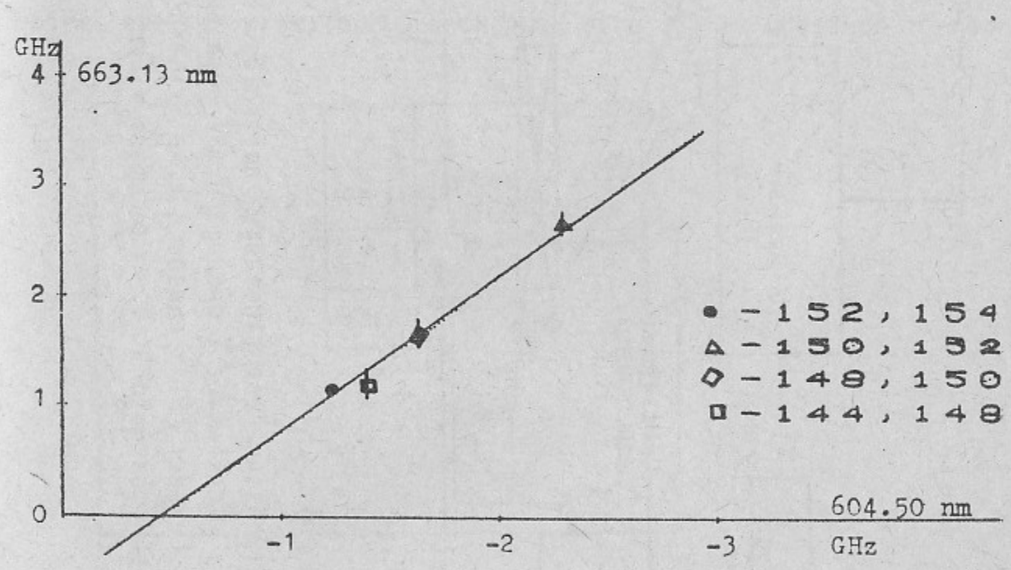

Fig.7. Examples of King plots. Measured IS values are plotted versus IS in a pure 6s->6p transition 604.50 nm. The gradient is the ratio of the field shifts on two lines, intercept depends on the mass shift.

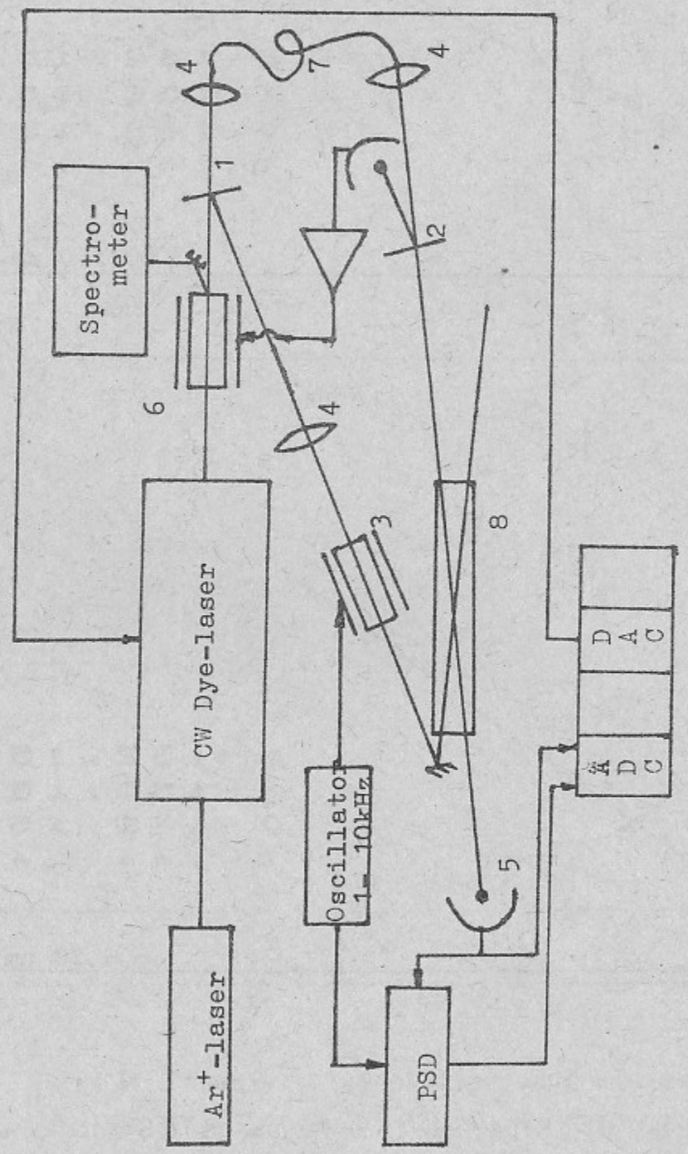

Fig.8. Saturation spectroscopy apparatus. 1,2 - beam splitters; 3 - a Pockels cell producing the pump beam intensity modulation; 4 - lenses; 5 - photodiode; 6 - intensity stabilizing Pockels cell modulator; 7 - monomode fiber; 8 - samarium cell.

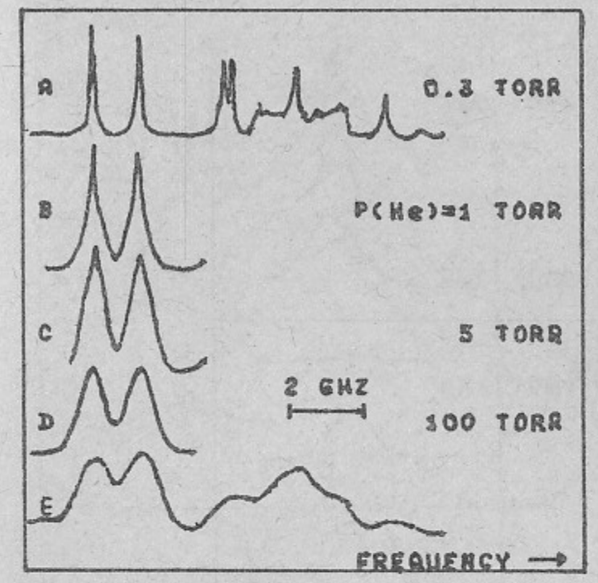

Fig.9. Recordings of the 656.35 nm E1-transition from the ground term. A-D - saturation spectroscopy lineshapes at different buffer gas pressures. E - linear absorption recorded at 0.3 Torr of He. Peak absorption - about 60%. The linear absorption lineshape was practically unchanged upon the He pressure increase up to 100 Torr

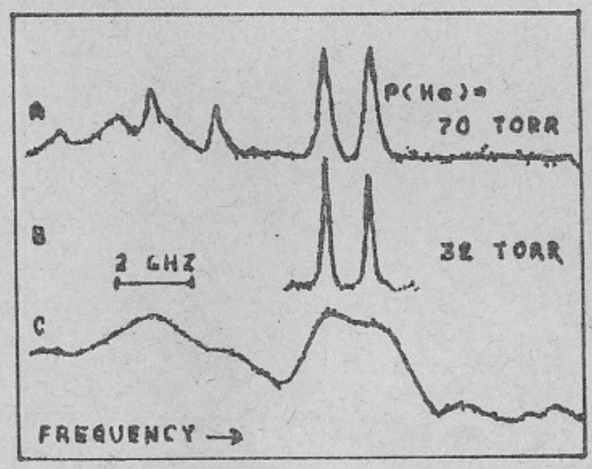

Fig.10 The 643.76 nm transition from an excited state. A, B - saturation spectroscopy lineshapes; C - linear absorption at 70 Torr of He. Peak absorption - about 50%.

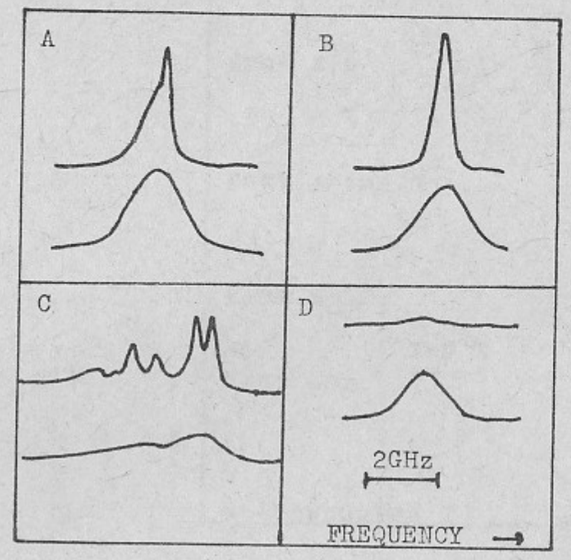

Fig.11. Recordings of M1-candidates: A - 645.20 nm; B - 645.75 nm; C - 645.93 nm; D - 661.95 nm. Upper curves - saturation signals, lower curves - linear absorption. Helium pressure - 25 Torr.

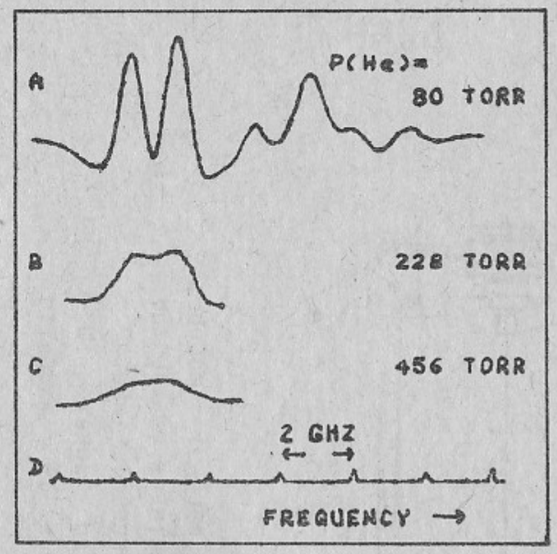

Fig.12. Pressure broadening of a typical samarium transition 656.35 nm. A-C - Faraday rotation, H=100 Oe; D - transmission through a reference cavity.

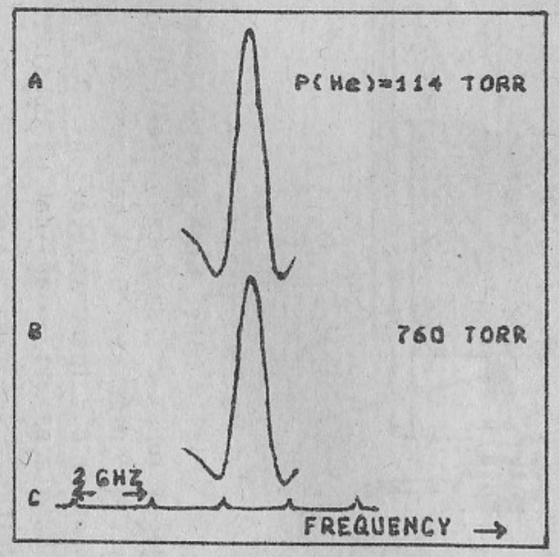

Fig.13. The 661.95 nm transition. A,B.- Faraday rotation; C.- transmission through a reference cavity. No manifestations of pressure broadening can be seen in the figure.

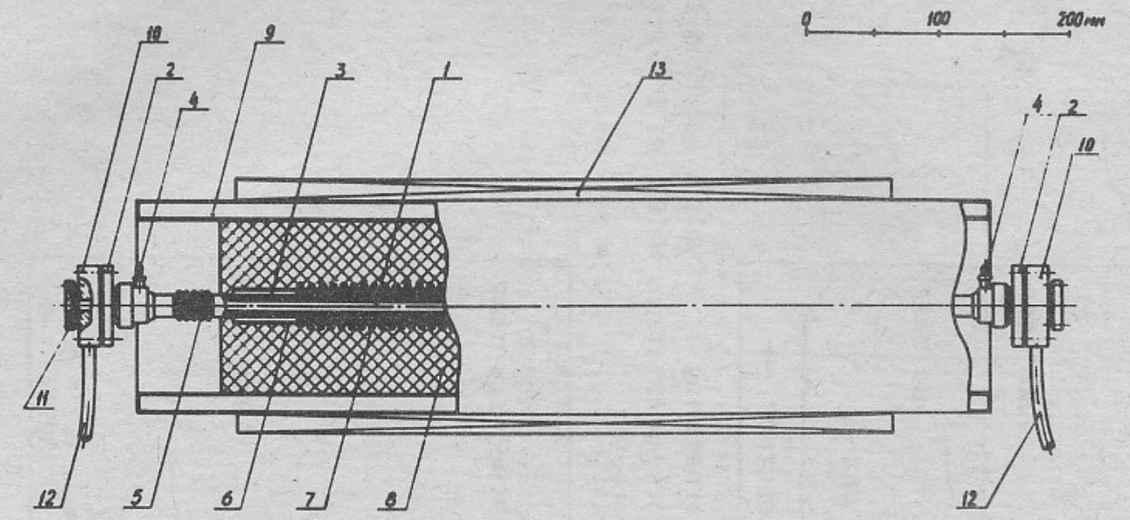

Fig.14. The high pressure samarium vapor cell. 1 - molybdenum tube; 2 - stainless steel flanges; 3 - stainless steel tube; 4 - nipples; 5 - bellows; 6 - electric-porcelain tube; 7 - heater; 8 - thermoinsulation; 9 - water-cooled jacket; 10 - end-pieces; 11 - optical windows; 12 - gas leads; 13 - magnetic coil.

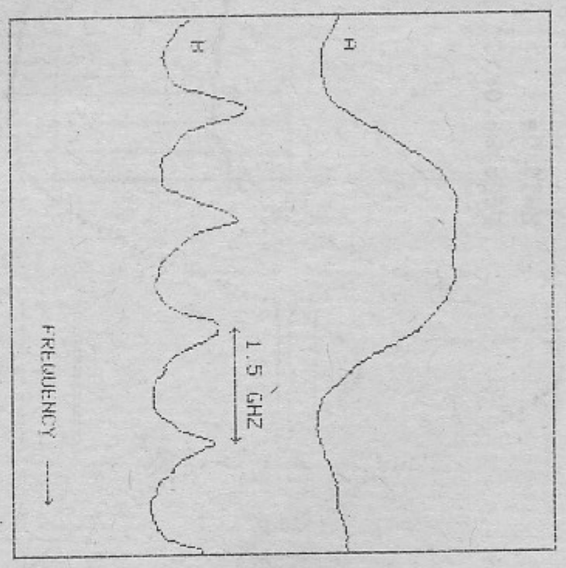

Fig.15. A - Faraday rotation on the 569 nm M1-transition at H≈700 Oe. B - transmission through a reference cavity.

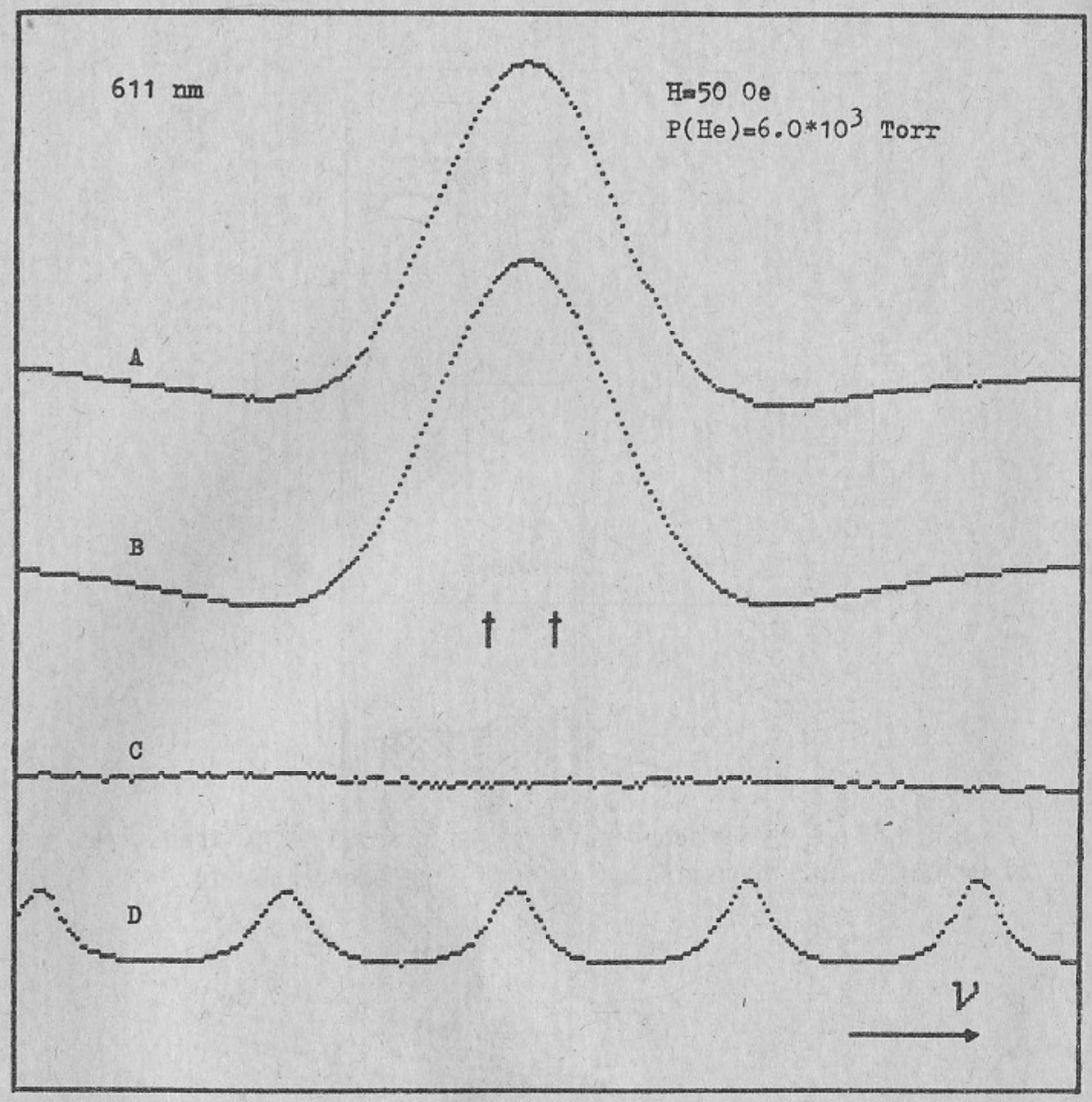

Fig.16. A - measured Faraday rotation lineshape for the $^7F_3 \rightarrow {}^5D_2$ M1-transition 611 nm. Peak rotation ≈7 mrad. B - fitting curve with the parameters: γ=1.1 GHz, Δ_D=650 MHz. Arrows mark the positions of "effective isotopes". C - difference of the curves A and B. D - transmission through a reference cavity with FSR=1.50 GHz.

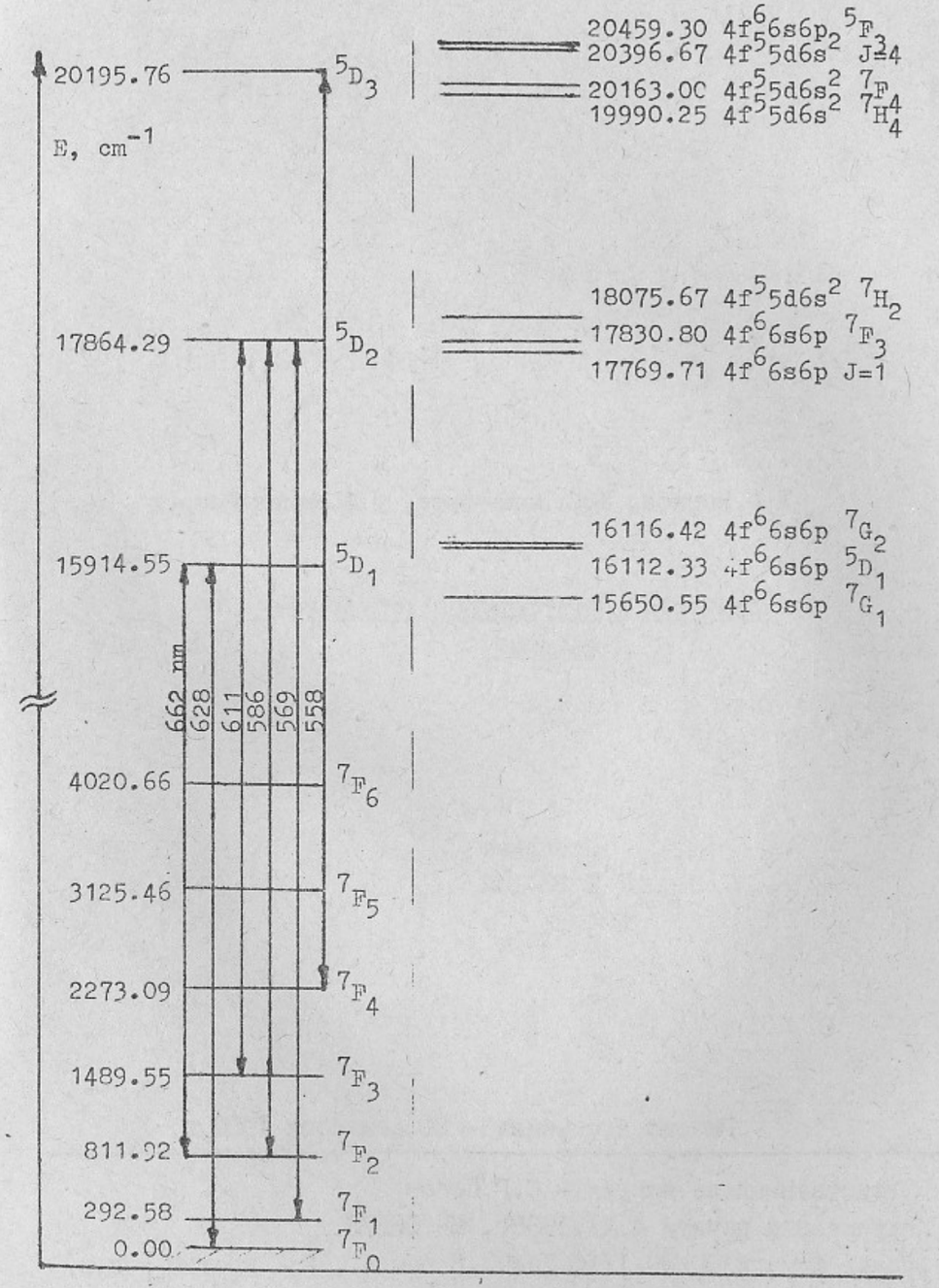

Fig.17. The $4f^6 6s^2$ levels of SmI and the opposite parity levels with $\Delta J=0,\pm1$ lying close to them ($|\Delta E|<300$ cm^{-1}). Also indicated are the M1-transitions observed in this work.

Л.М.Барков, М.С.Золоторев, Д.А.Мелик-Пашаев

ЛАЗЕРНАЯ СПЕКТРОСКОПИЯ АТОМАРНОГО САМАРИЯ

Препринт
№ 88-142

Работа поступила - 28 сентября 1988 г.

Ответственный за выпуск - С.Г.Попов
Подписано к печати 4.XI.1988г. МН 08572
Формат бумаги 60x90 1/16 Усл.3,5 печ.л., 2,8 учетно-изд.л.
Тираж 290 экз. Бесплатно. Заказ № 142.

Ротапринт ИЯФ СО АН СССР, г.Новосибирск, 90